



Ultrafast transient liquid assisted growth of $\text{YBa}_2\text{Cu}_3\text{O}_7$: a new scenario for enhanced vortex pinning

Xavier Obradors

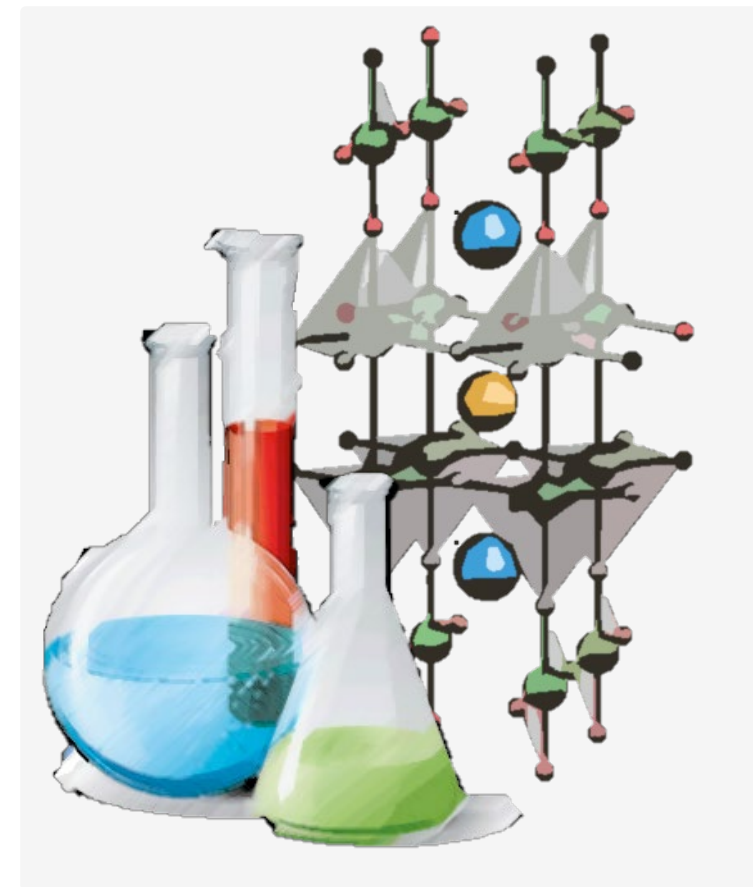
T. Puig¹, J. Banchewski¹, S. Rasi^{1,2}, A. Queralto¹, K. Gupta¹, L. Saltarelli¹, D. Garcia^{1,3}, A. Pacheco¹, R. Vlad¹, L. Soler¹, J. Jareño¹, R. Guzmán¹, N. Chamorro^{3,1}, M. Sieger¹, S. Ricart¹, J. Farjas², P. Roura², C. Mocuta⁴, R. Yanez³, J. Ros³

¹ Institut de Ciència de Materials de Barcelona, ICMAB-CSIC, Catalonia, Spain

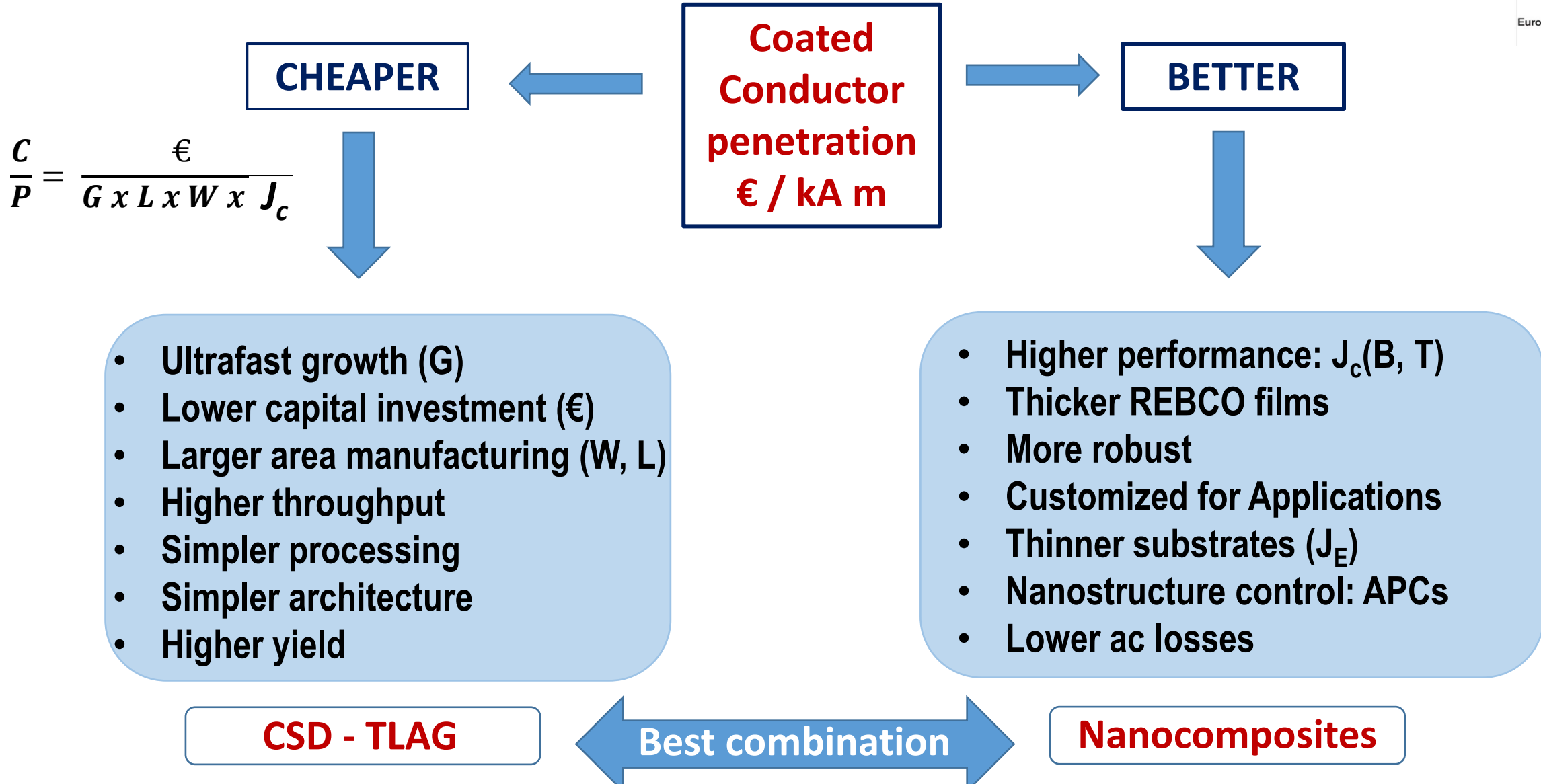
² GRMT, Department of Physics, University of Girona, Girona, Catalonia, Spain

³ Departament de Química, Univ. Autònoma de Barcelona, Catalonia, Spain

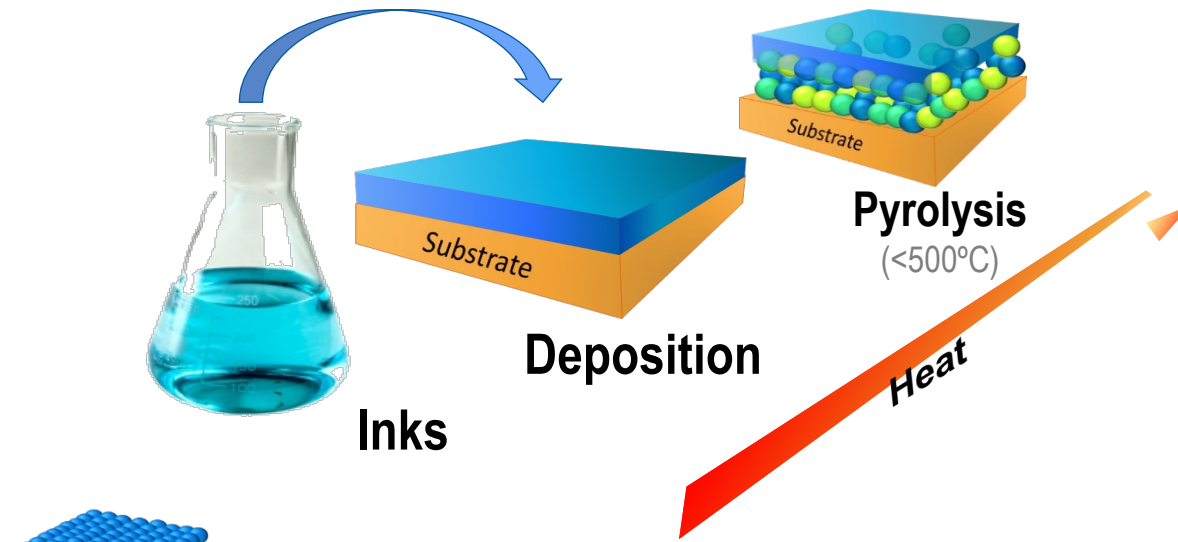
⁴ Diffabs beamline, Soleil Synchrotron, Paris, France



Coated Conductors: materials objectives



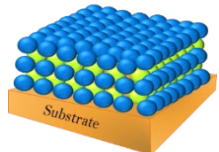
Chemical Solution Deposition (CSD)



X. Obradors et al., SUST (2012); SUST (2018)
C. Pop, SUST (2019); B. Vallejo, J Mat Chem C (2020)

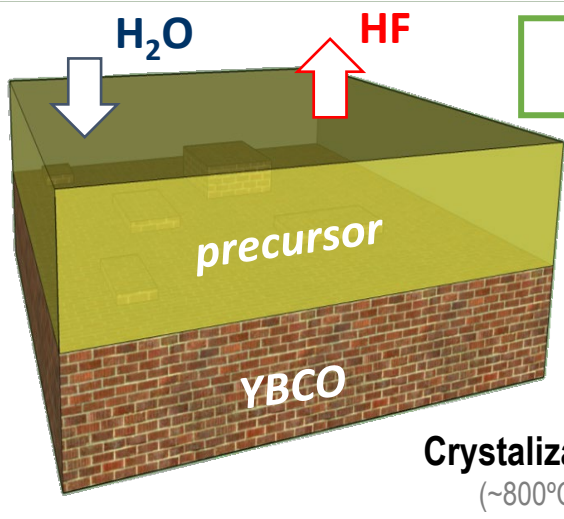
First step

- Inks (Trifluoroacetates, low Fluorine)
- Non-vacuum deposition
- Colloidal solutions for nanocomposites
- Industrially scalable: low cost manufacturing

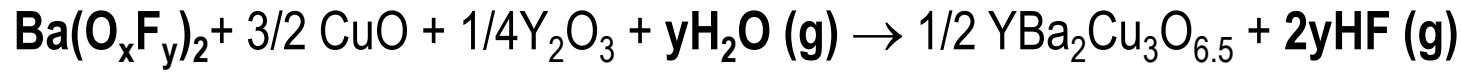


Trifluoroacetate-route: Low Fluorine TFA metalorganic precursors

Gas-Solid reaction

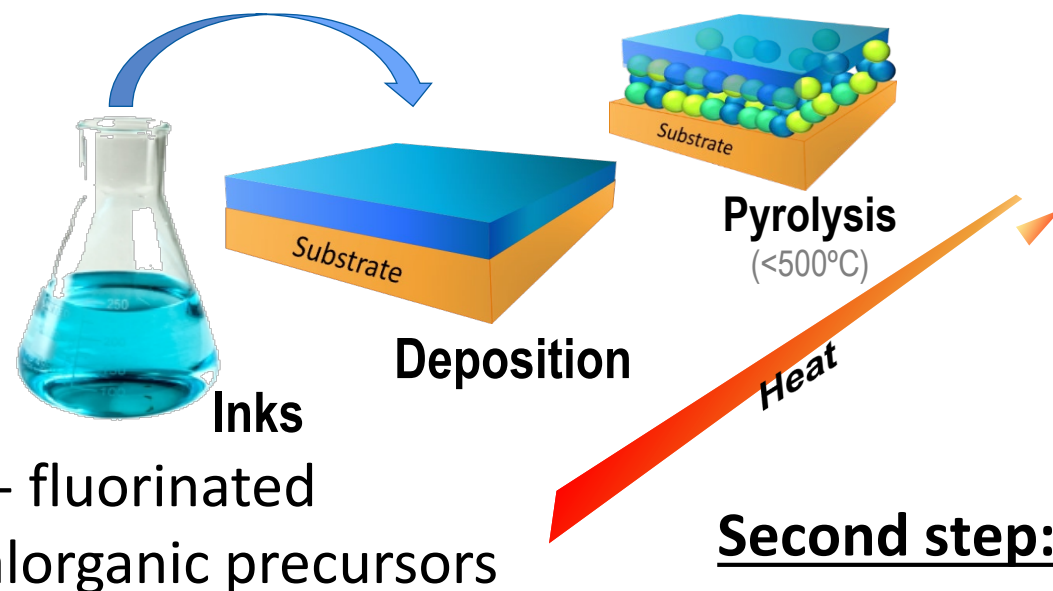


Second step: film growth



- Supersaturation conditions highly dependent on P_{HF} and $P_{\text{H}_2\text{O}}$
- Growth rate for c-axis growth limited to $\approx 1\text{nm/s}$
- High performances ($I_c=400 \text{ A/cm-w}$)
- Complicated R2R gas flow furnaces

CSD – Transient Liquid Assisted Growth

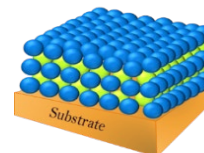


- L. Soler et al., Nat Comm (2020)*
- S. Rasi et al., J. Phys Chem C (2020)*
- S. Rasi et al., Adv Sci (2022)*
- L. Saltarelli, ACS Appl Mat Int (2022)*

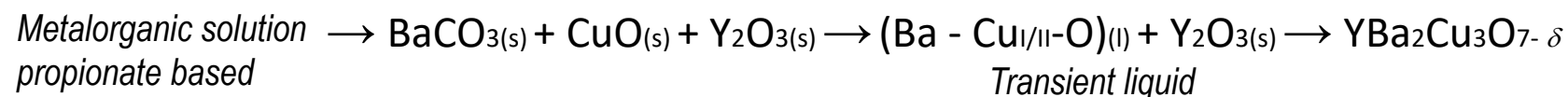
First step

- Inks (Non-Fluorine)
- Non-vacuum deposition
- Colloidal solutions for nanocomposites
- Industrially scalable: low cost manufacturing

Second step: TLAG film growth



Crystalization
($\sim 800^{\circ}\text{C}$)



Coated Conductor manufacturing (1-2 μm)

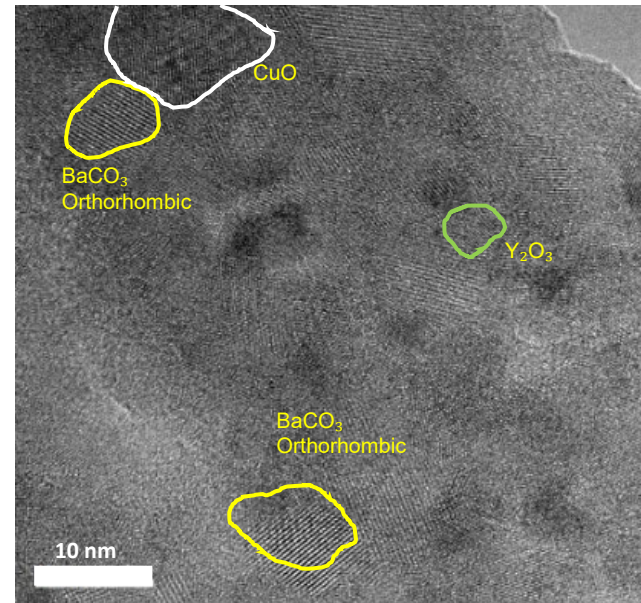
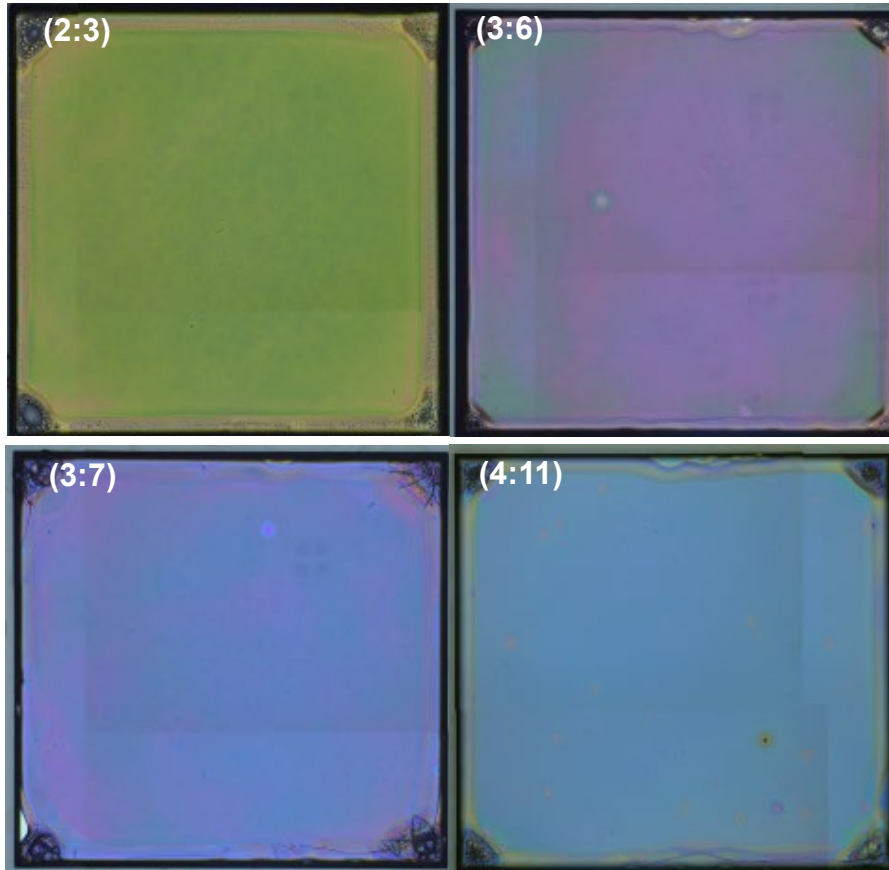
- Typical growth time TFA: 30-60 min
- Typical growth time TLAG: 5-10 s
- Throughput TFA: 5-10 m/h
- Throughput TLAG: 3.000 -4.000 m/h

- ❖ *Non-equilibrium process: kinetic control*
- ❖ *Liquid-solid conversion reaction (high atomic diffusion in liquids)*
- ❖ *Supersaturation degree can be controlled through Ba:Cu ratio*
- ❖ *Ultrafast growth rates $>100 - 1.000 \text{ nm/s}$*
- ❖ *Simplified R2R large area reactor for industrial manufacturing*
- ❖ *Environmentally friendly*

See T. Puig: 4MOr1C-01 (9:00 am)

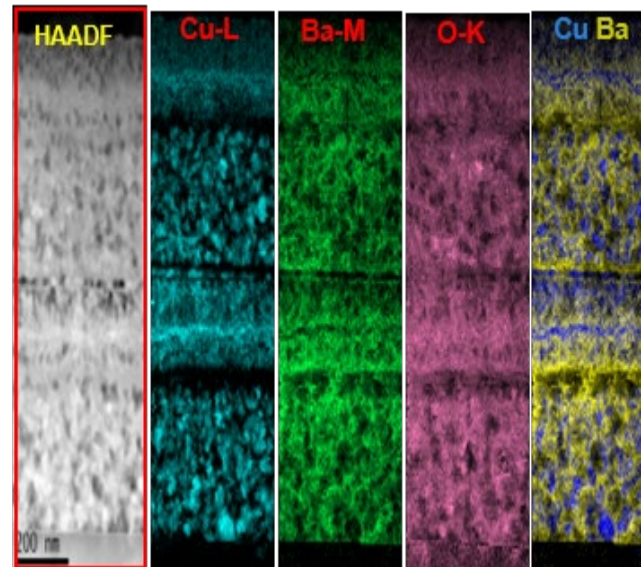
Pyrolyzed F-free CSD films

- ✓ Propionate precursors + additives
- ✓ Optimised solutions of *various stoichiometries* yield homogeneous nanocrystalline layers



- ✓ Reduced sizes of the nanocrystalline YBCO precursors favour greatly atomic mobility, enabling *ultrafast growth rates*

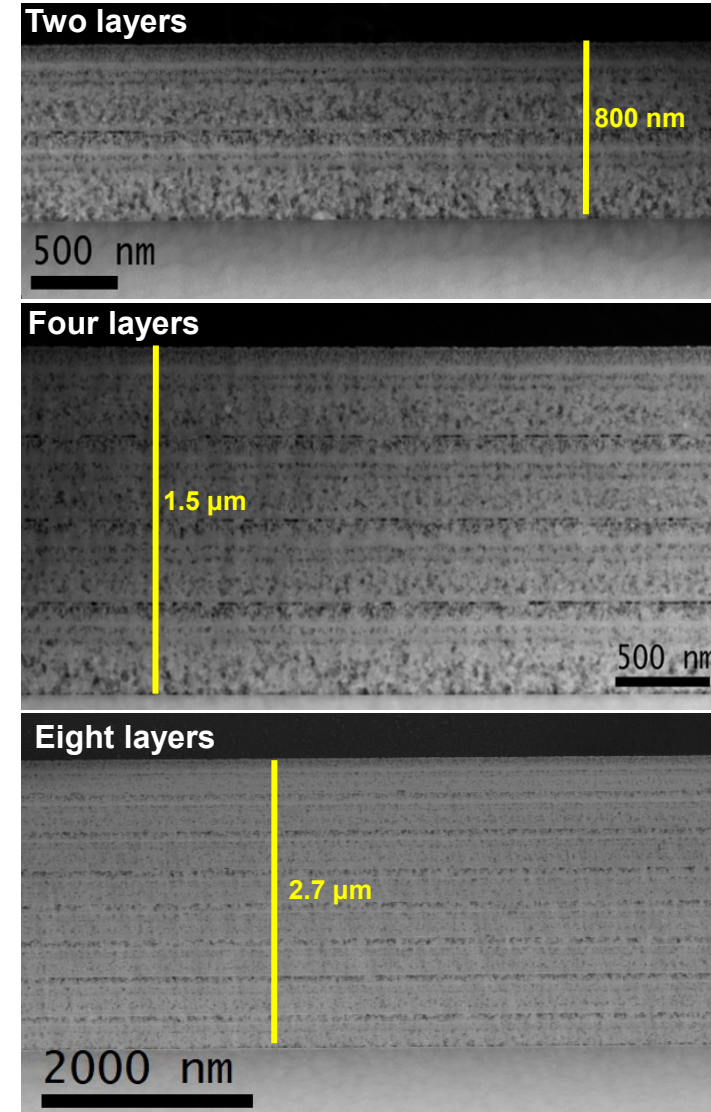
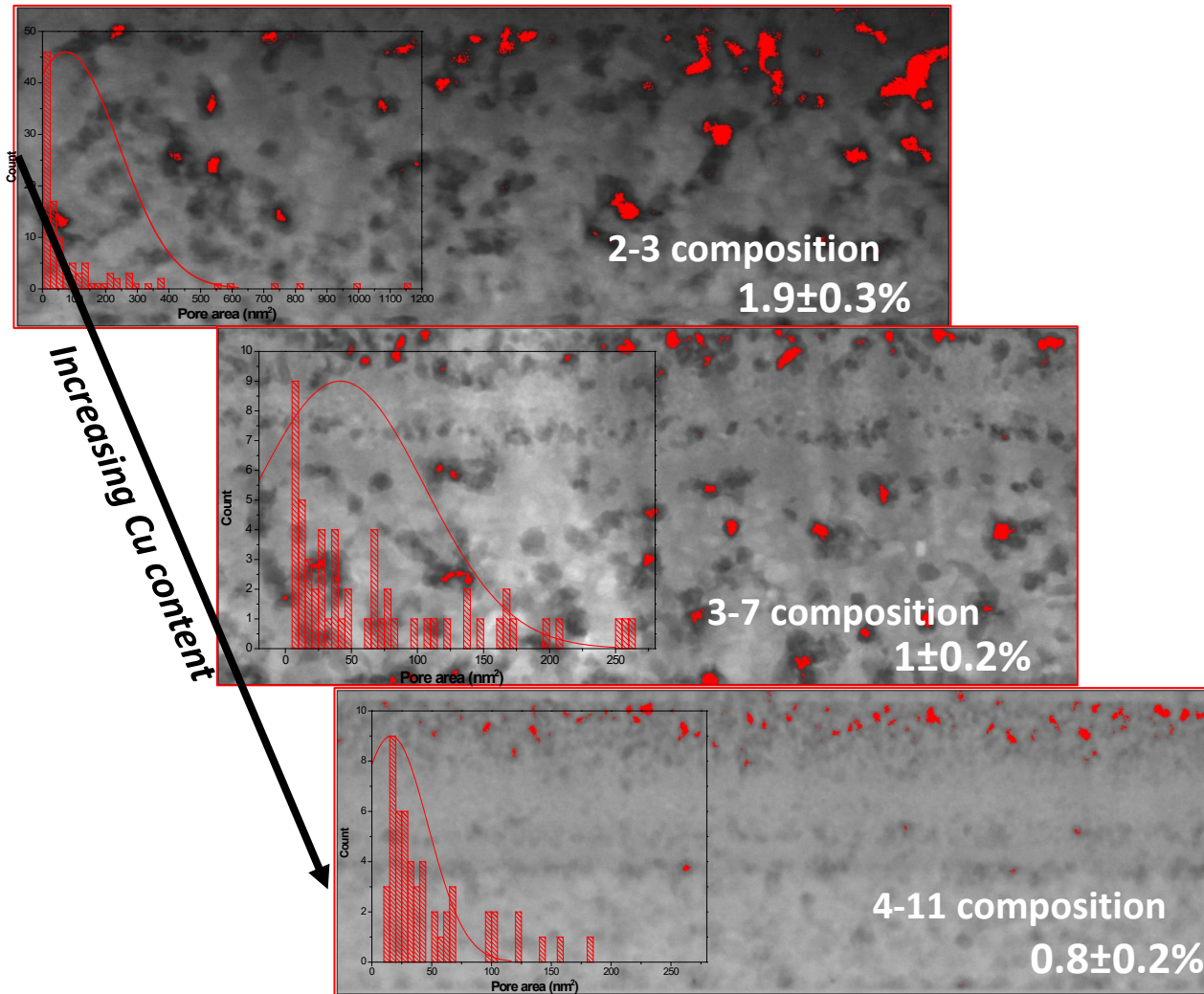
BaCO₃ (orthorhombic): 10 - 30 nm
CuO: 10 - 25 nm
Y₂O₃: 5 - 6 nm



- ✓ *Nanoscale homogeneous* distribution of the phases throughout the layer

Pyrolyzed F-free CSD films

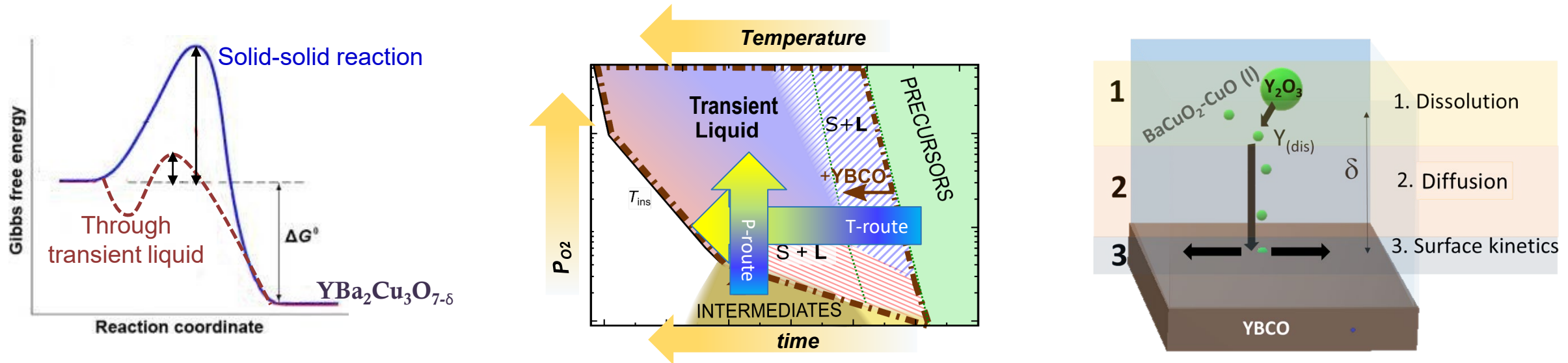
- ✓ *Low porosity* of the layers, decreasing with the increase of the composition's Cu content



- ✓ Suitability for *multideposition* with no loss in homogeneity

Transient Liquid Assisted Growth: TLAG-CSD

Non-equilibrium process kinetically controlled

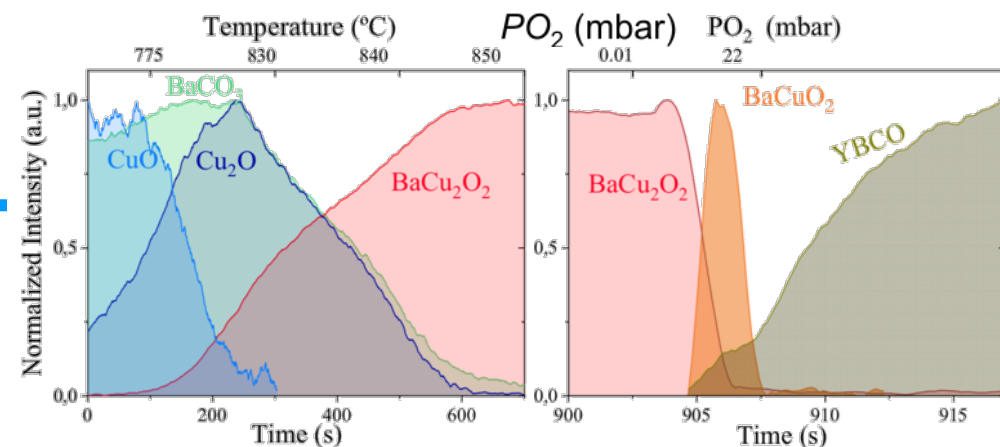
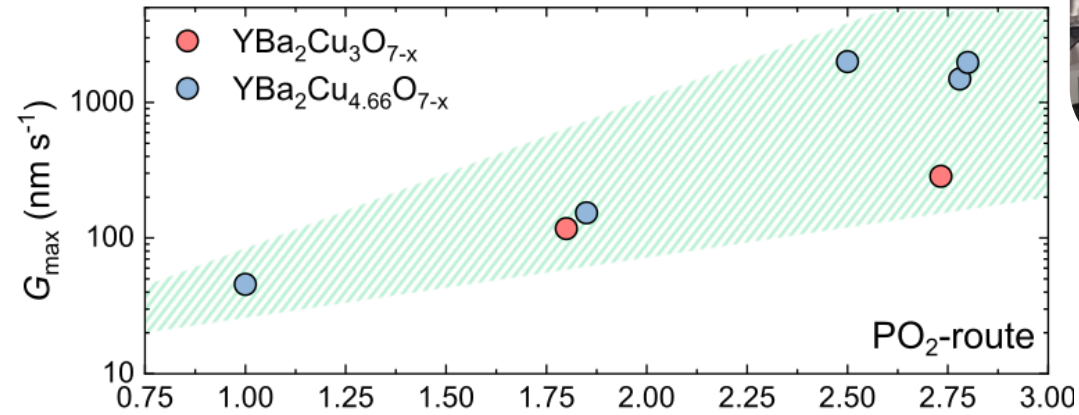
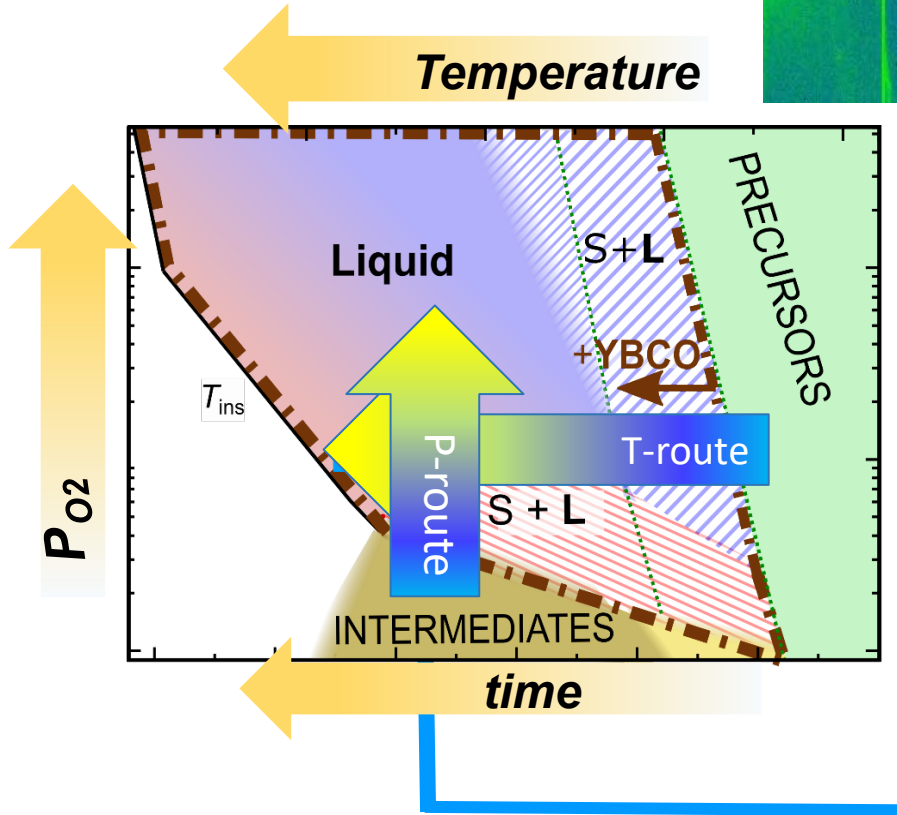
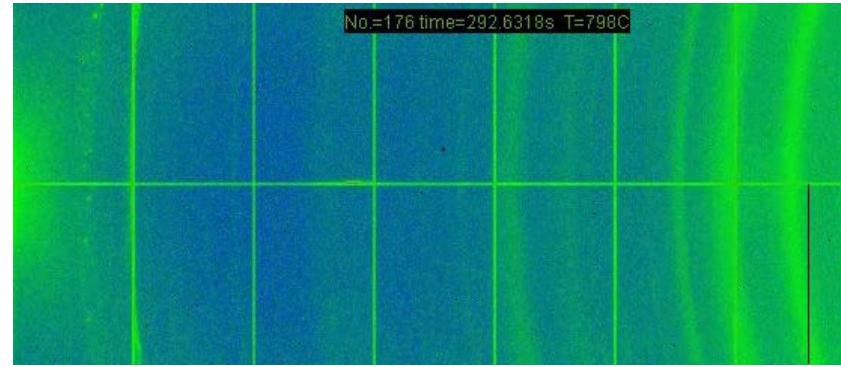
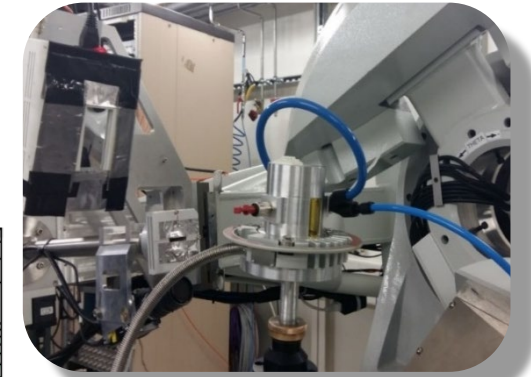


- Transient liquids (Ba-Cu-O) form much faster than the equilibrium solid phase (YBCO)
- No need of equilibrium liquid phases in the phase diagram

- RE solubility in the liquid controls supersaturation
- Ultrafast growth rates working at high supersaturation

Kinetic process and intermediate phases

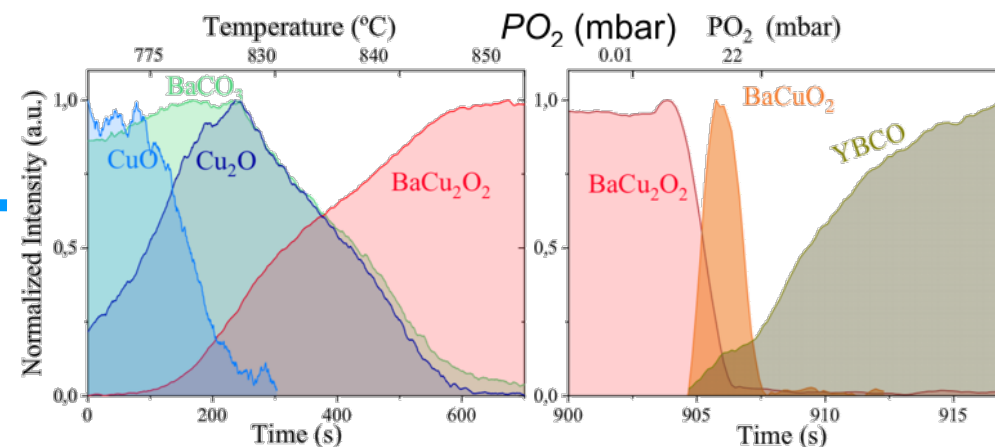
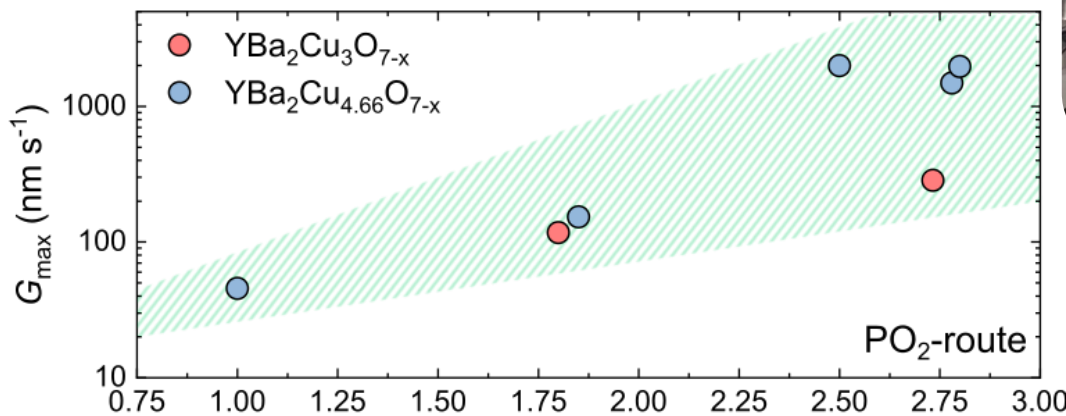
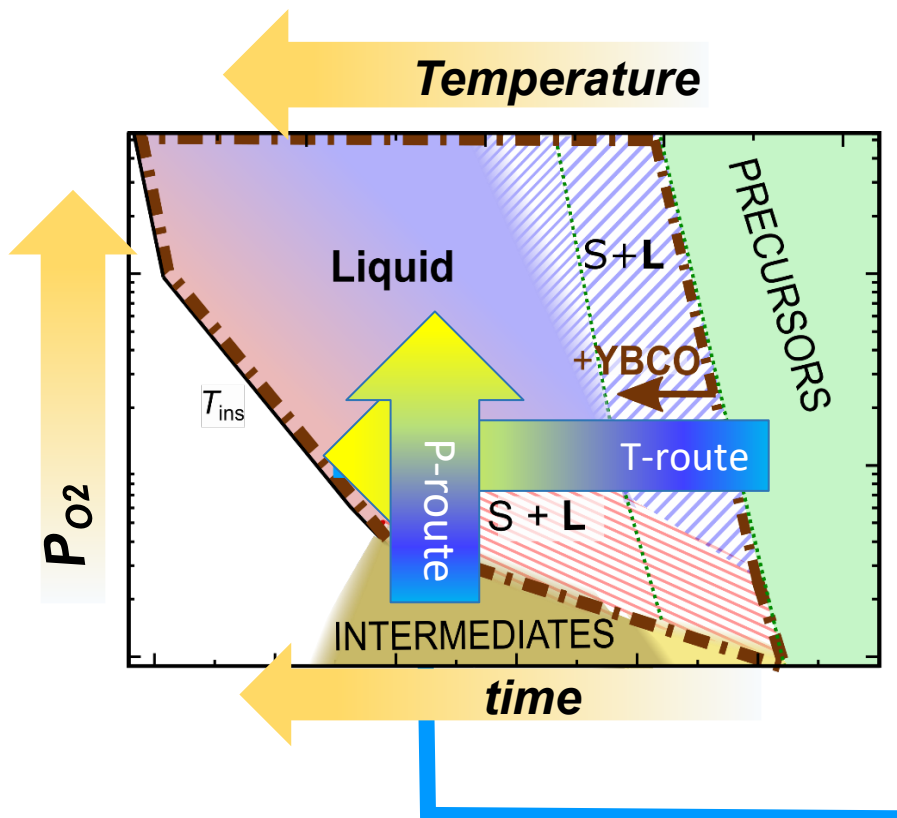
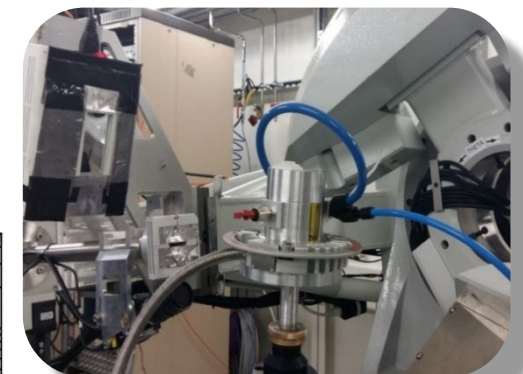
In-situ XRD synchrotron exp.
from 100 ms down to 2 ms
acquisition time



T, P_{O2}, P_{Total}
T-ramp
P-ramp
Liquid composition
Rare Earth

Kinetic process and intermediate phases

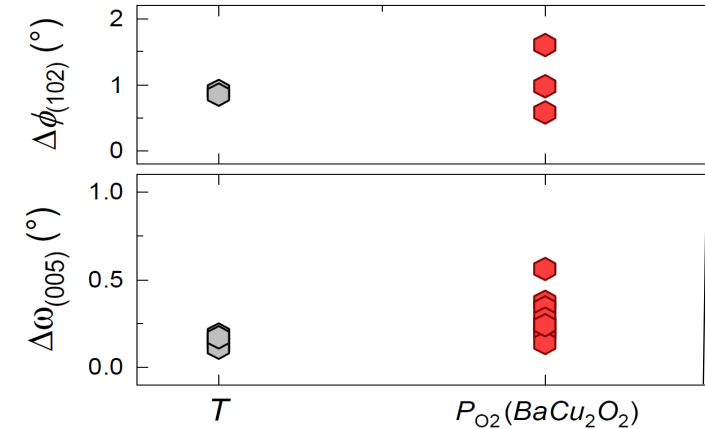
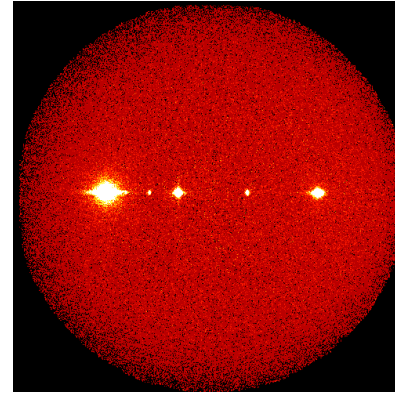
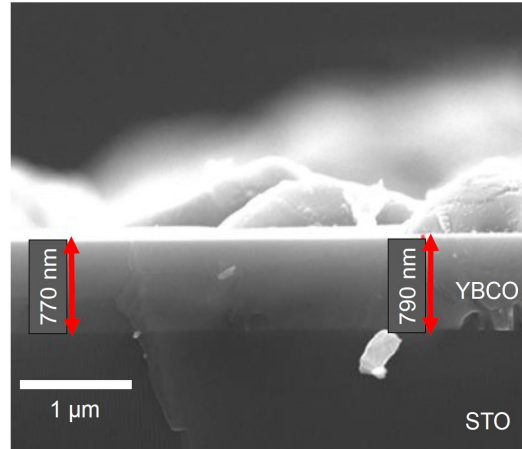
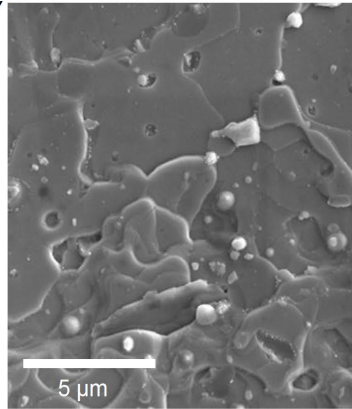
In-situ XRD synchrotron exp.
from 100 ms down to 2 ms
acquisition time



T, P_{O_2}, P_{Total}
T-ramp
P-ramp
Liquid composition
Rare Earth

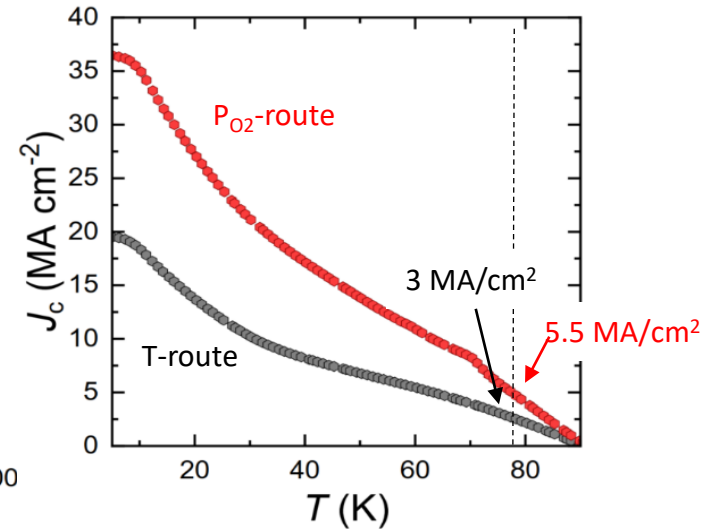
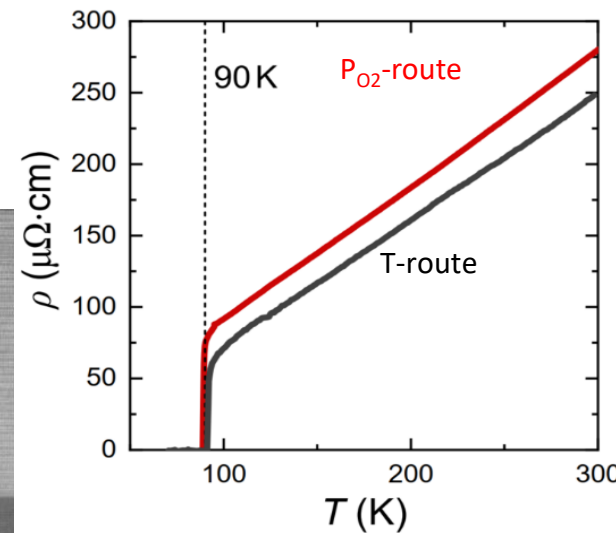
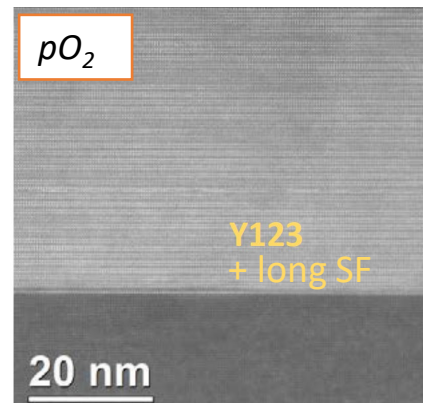
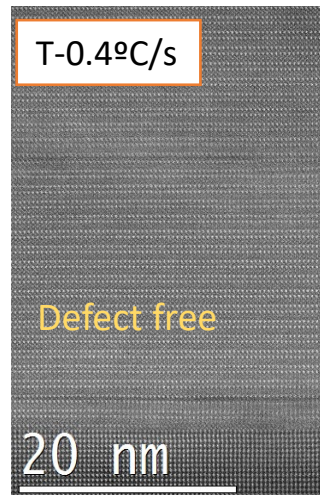
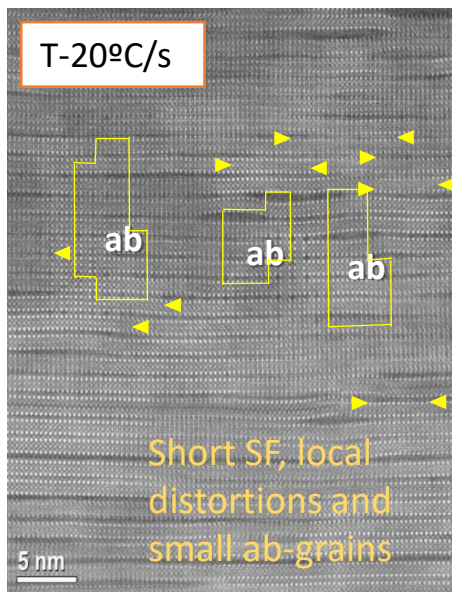
TLAG-CSD films: microstructure and properties

Extremely low porosity and highly epitaxial YBCO grown layers



Tunable microstructure: depends a lot on process conditions

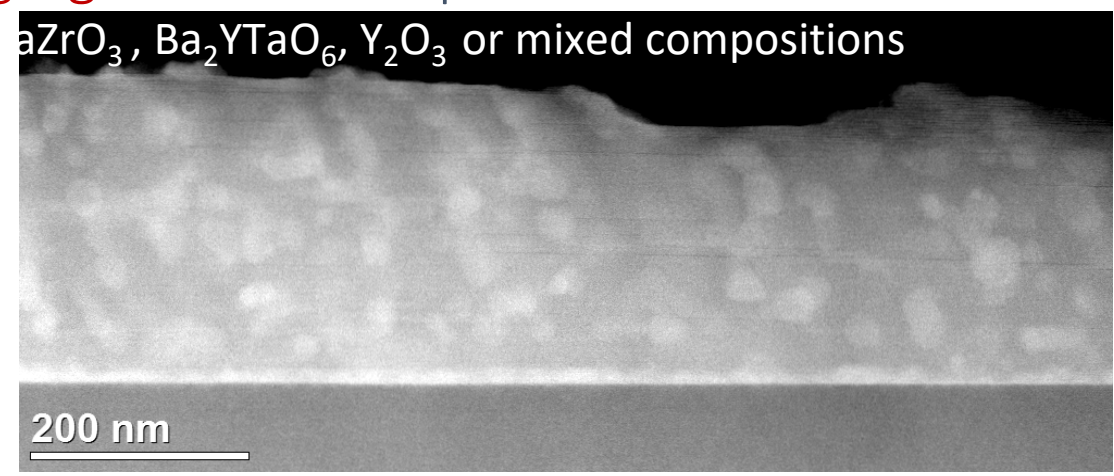
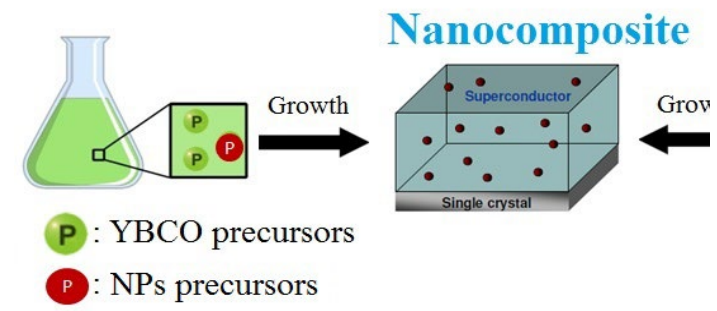
High performance demonstrated



ss-Nanocomposites: Not suitable for TLAG

Use of complex solutions for **spontaneous segregation** of nanoparticles

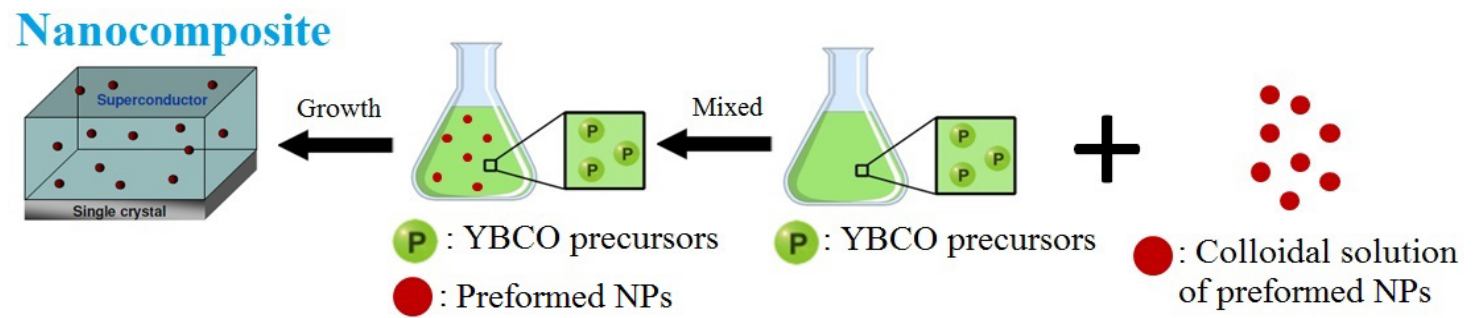
(BaZrO₃, BaHfO₃, Ba₂YTaO₆, BaCeO₃)



- J. Gutierrez et al, Nat Mat (2007);
- A. Llordés et al, Nat Mat (2012)

pn-Nanocomposites: Colloidal solutions with **preformed nanoparticles** (N. Chamorro, RSC Adv. (2020))

Suitable for TFA and TLAG



- Spinel (MFe₂O₄)
- Fluorite (CeO₂, ZrO₂)
- Perovskite BaMO₃ (M= Zr, Hf)
- Bronze Ba(Ta,Nb)₂O₆

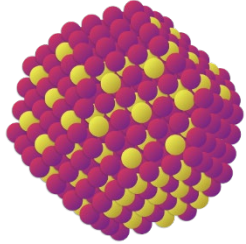
Need to stabilize np in the alcoholic and ionic environment of YBCO precursor solution at high concentrations

- P. Cayado et al, SUST (2015)
- X. Obradors et al, SUST (2018)
- D. Garcia et al., to be published

Nanoparticles for multifunctional colloidal solutions

Requeriments

NP solution

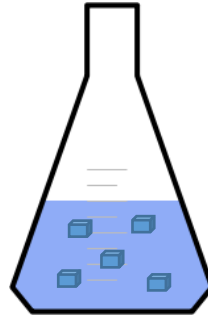


Small-size < 10 nm

Non-aggregation
in alcohol solution

High concentrations in
alcohol solution
(≥ 100 mM)

Stabilization in YBCO precursor solution



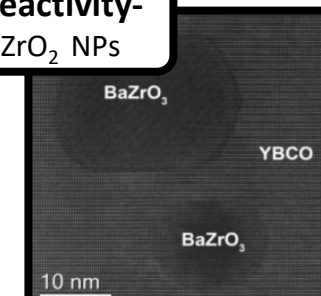
NPs compatible and stable in
YBCO precursor solution
-non- aggregation
-no precipitation

Compatibility with CSD-TLAG process

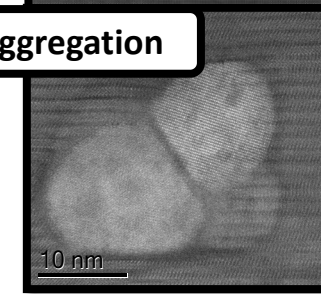
NP composition non-reactive
with YBCO

High-thermal stability of
NP composition

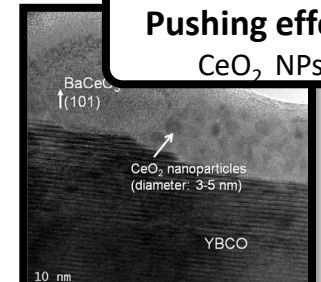
Reactivity-
ZrO₂ NPs



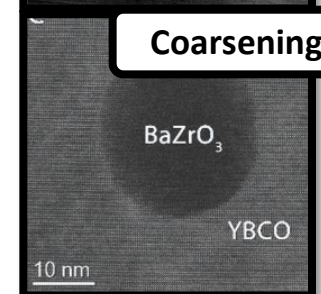
Aggregation



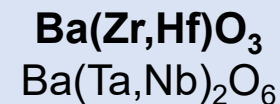
Pushing effect-
CeO₂ NPs



Coarsening



Multifunctional colloidal ink
(Patent EP22382741)



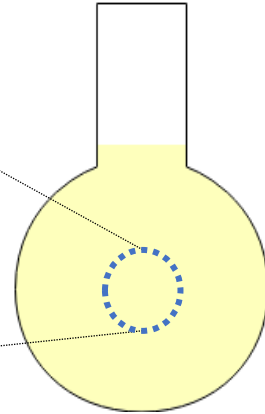
Nanoparticle synthesis process

Hybrid Hydrolitic-Solvothermal Synthesis (H2S2)

2 steps process for preformed BaMO₃ NP synthesis

1. Hydrolitic (sol-gel) step: nucleation

- **Metal precursor:**
Alcoxide M(OR)_x M=Zr,Hf, Ta or Nb
Hydroxide Ba(OH)₂ · 8H₂O
- **Stabilizer:** TREG
- **Solvent:** Alcohol media



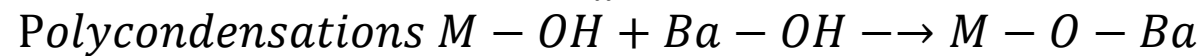
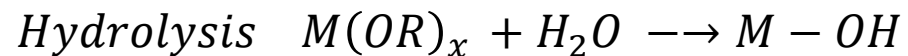
T, P



2. Solvothermal step: crystallization



Temperature < 250 °C
Reaction Time < 24h



Multifunctional colloidal ink
(Patent EP22382741)

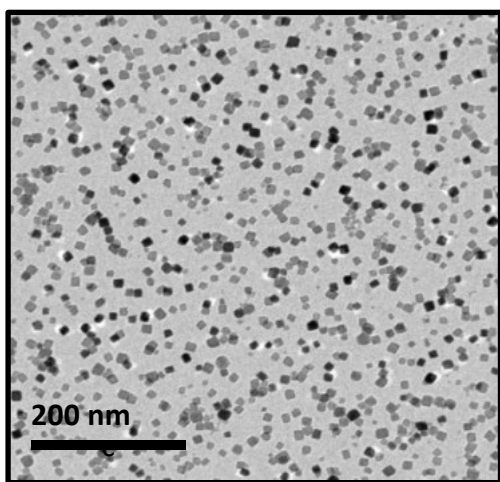
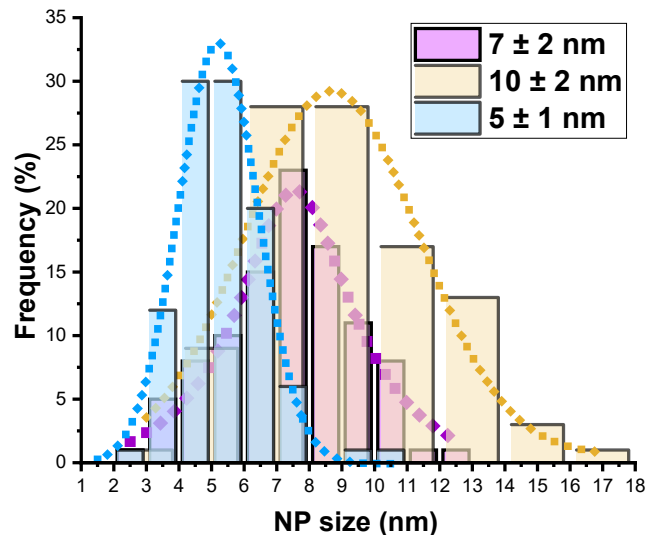
Limiting step: hydrolysis reaction

- ✓ Small sized NPs (3-15 nm)
- ✓ High NP concentrations (> 100 mM)
- ✓ Narrow range of size distribution: FWHM < 3nm
- ✓ Stable colloidal solutions (for months)



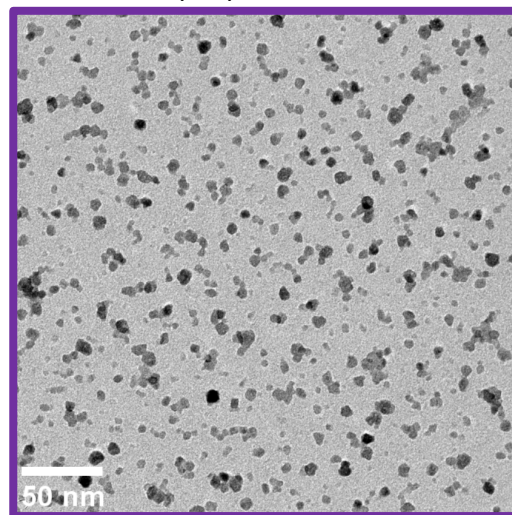
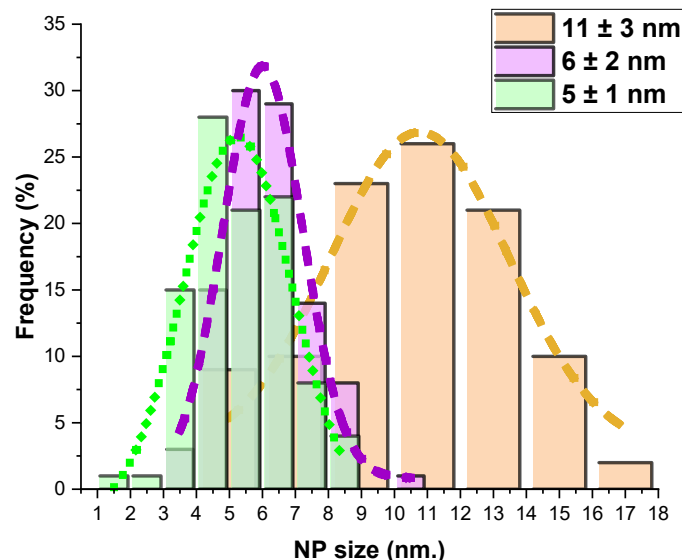
BaMO₃ (M= Zr and Hf) Nanoparticles

BaZrO₃ NC

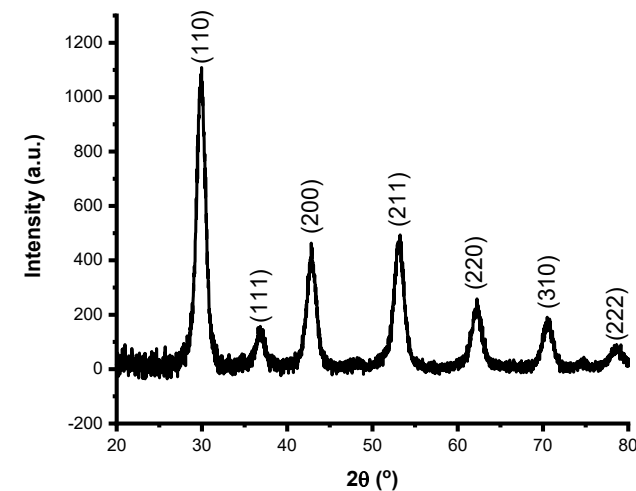
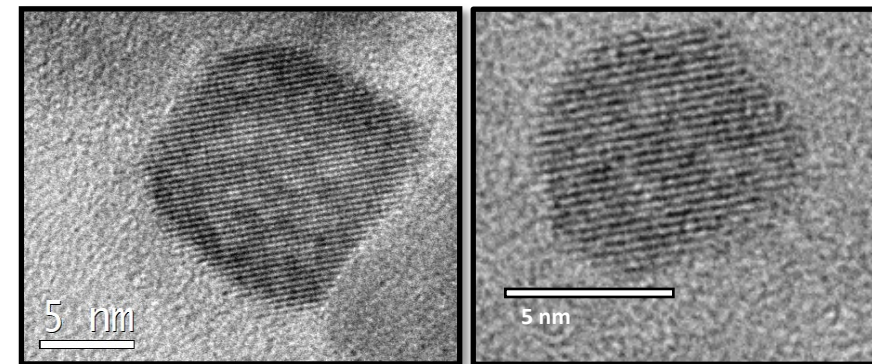


✓ Stable solutions (size/surface stability) for months

BaHfO₃ NC

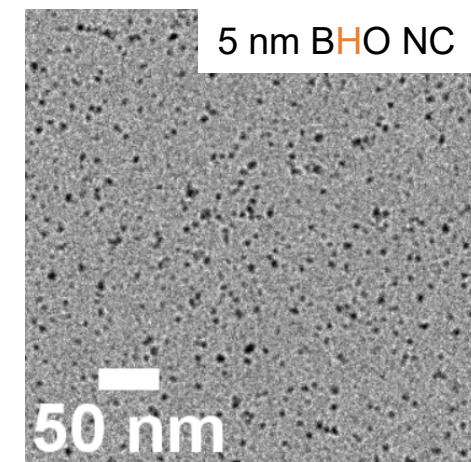
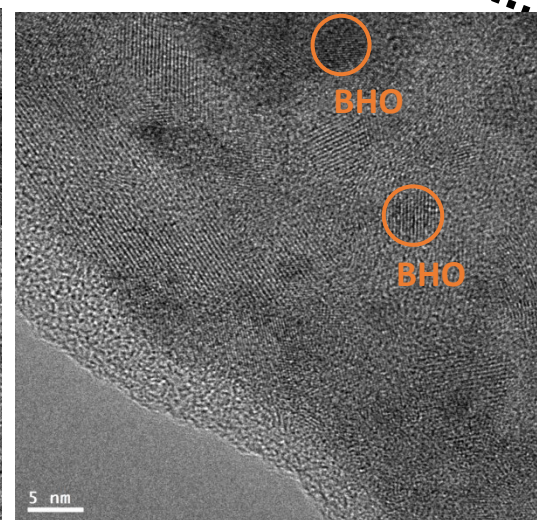
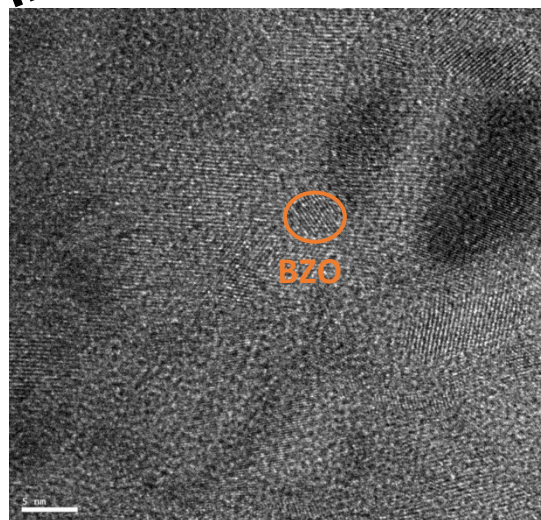
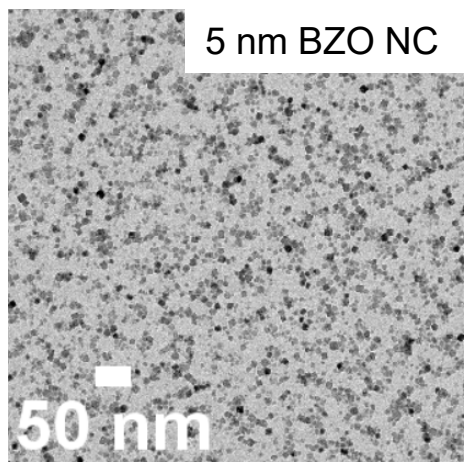
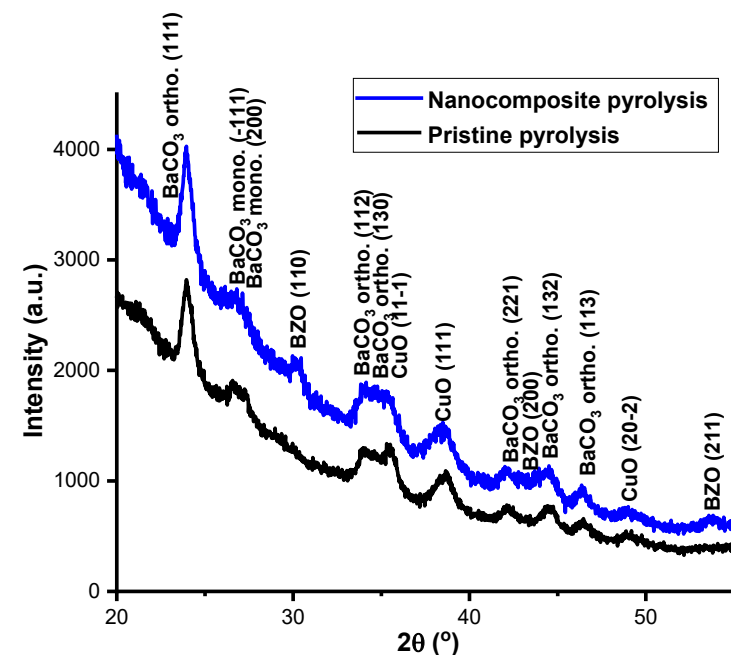
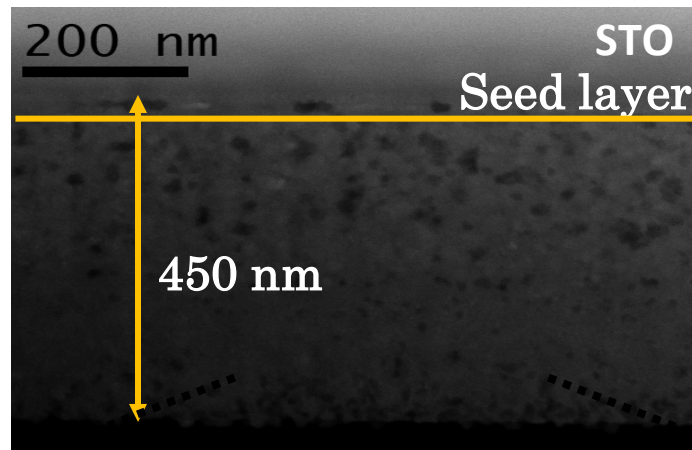
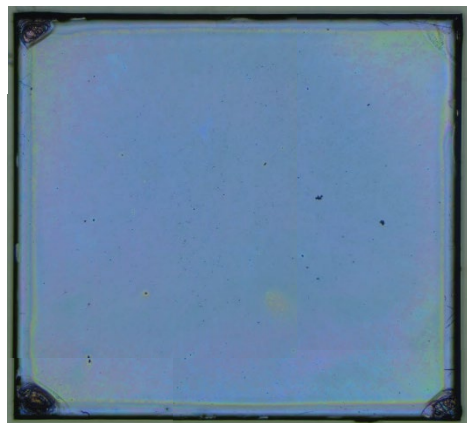


✓ Tuneable NP size from 4-20 nm



cubic phase

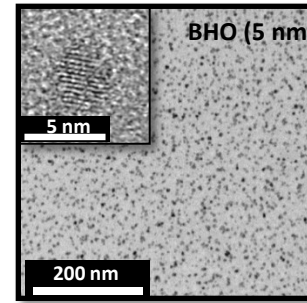
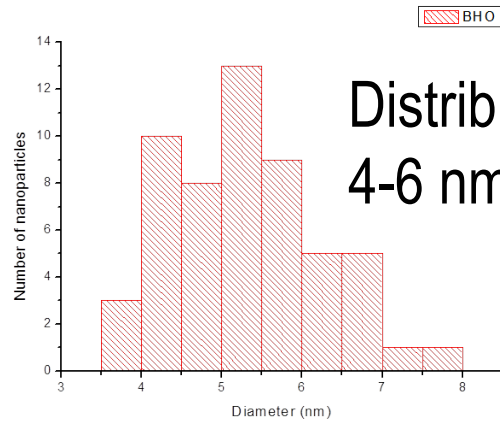
Nanocomposite pyrolysis



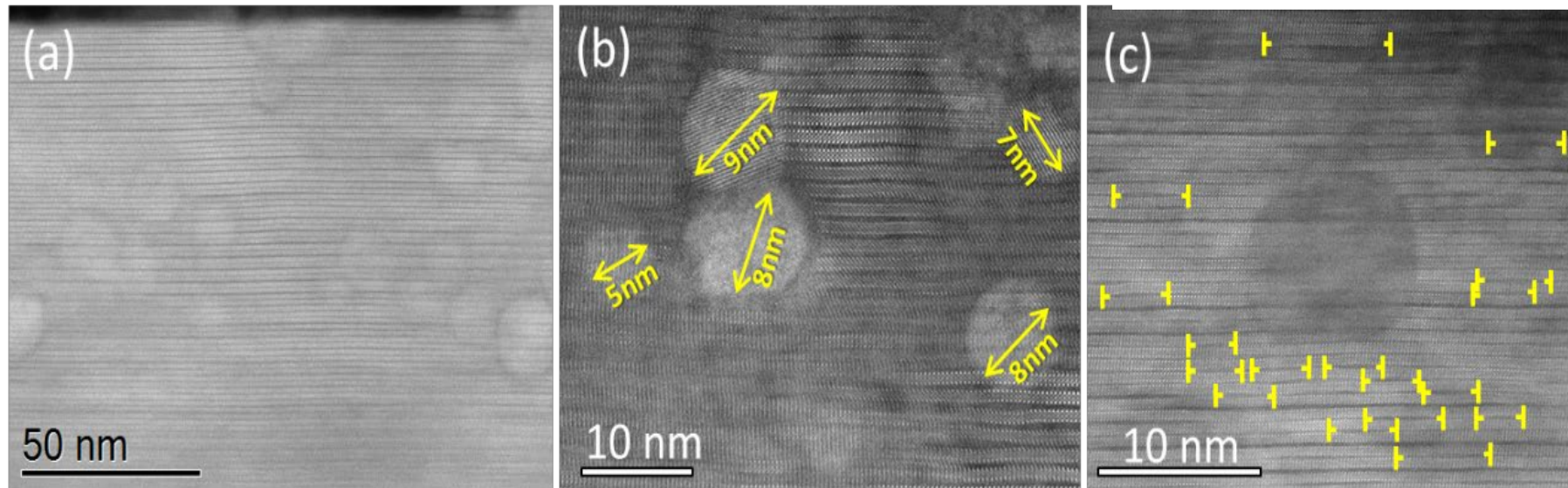
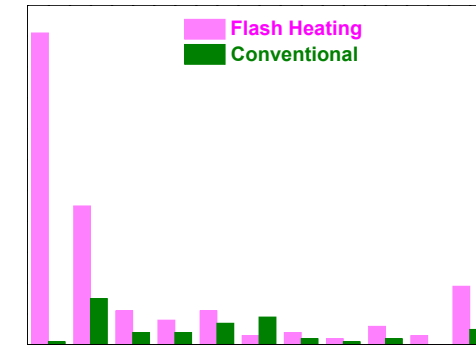
- ✓ Homogenous and reproducible multideposited films (up to 650 nm)
- ✓ Thickness of ~ 450 nm (1 pristine layer +1 layer with 12%mol of NPs)

- ✓ Crystalline NPs and no NP coarsening for 10 and 5 nm NPs.
- ✓ Same YBCO precursor phases as pristine

TFA-BHO pn-nanocomposites by Flash Heating



Flash heating (20 °C/s): 20%M BHO (5 nm)



$n_{np} \approx 40 \times 10^{22} \text{ m}^{-3}$ (x2,5) ($\approx 8 \%$ vol)

NPs random fraction: 94%

Short SFs are promoted! (20 – 30 nm)

Vol density partial dislocation: $\approx 2.3 \%$ vol (+ 60 %)

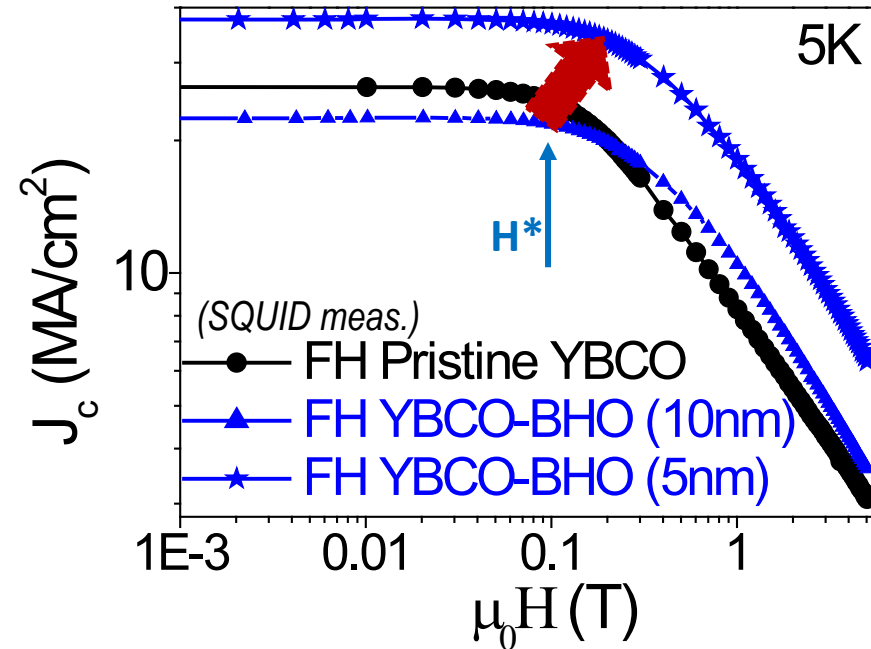
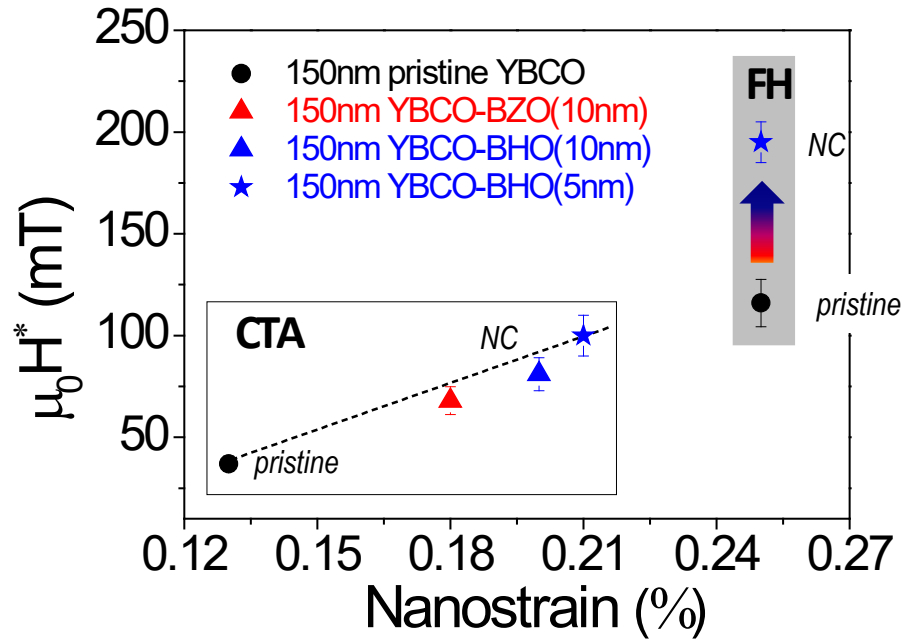
- Flash Heating strongly avoids NP coarsening
- Higher concentration of short stacking faults: higher density of partial dislocations
- NP size very close to the optimal size for vortex pinning (5-8 nm)

Z. Li et al, *Sci Rep.* (2019)

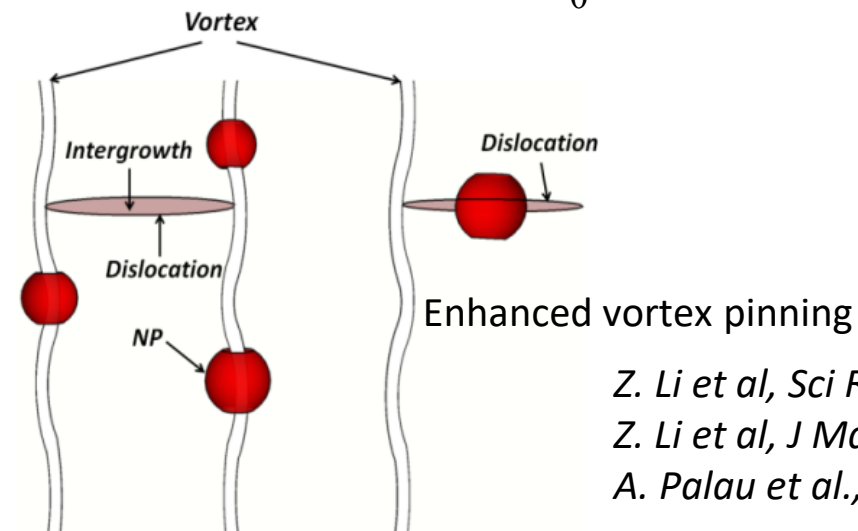
J Mat Chem C (2019)

Synergistic combination of Nps and nanostrain: enhanced vortex pinning

CTA: Conventional Thermal Annealing (0.4 °C/s)
FH: Flash heating (20°C/s) - Enhanced vortex pinning



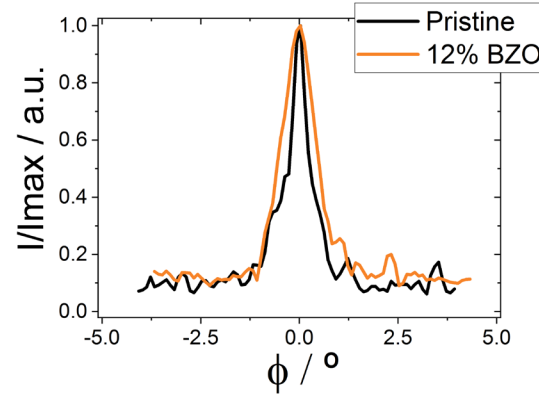
A leap increase of H^* beyond nanostrain NP diameter $\sim \xi_{ab}$ (coherence length)



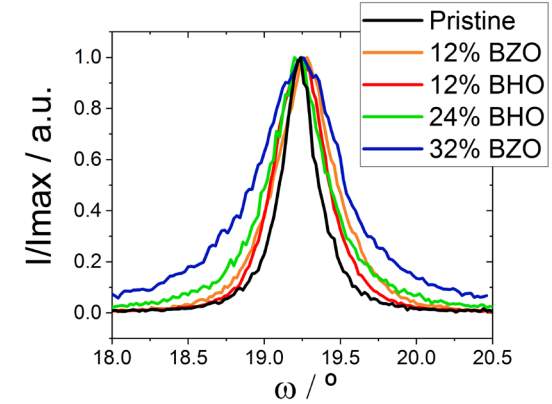
Z. Li et al, *Sci Rep.* (2019)
 Z. Li et al, *J Mat Chem C* (2019)
 A. Palau et al., *SUST* (2018)

Nanostrain & NPs (4-8 nm) Synergistic effect for enhanced vortex pinning

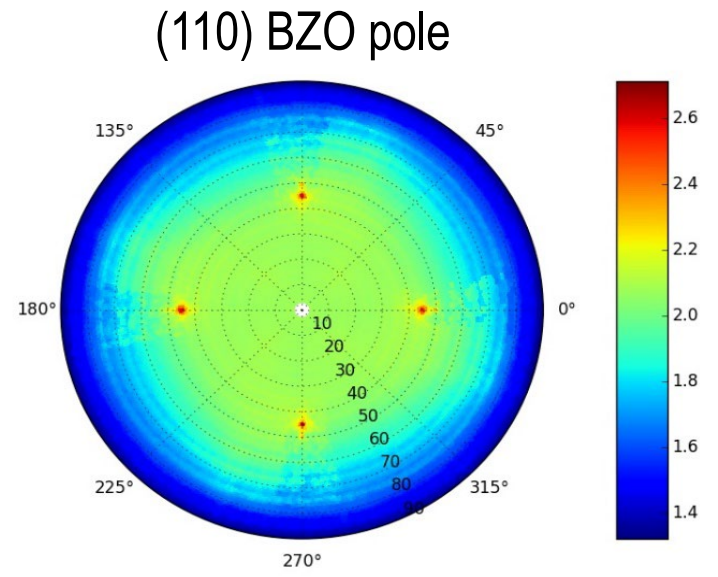
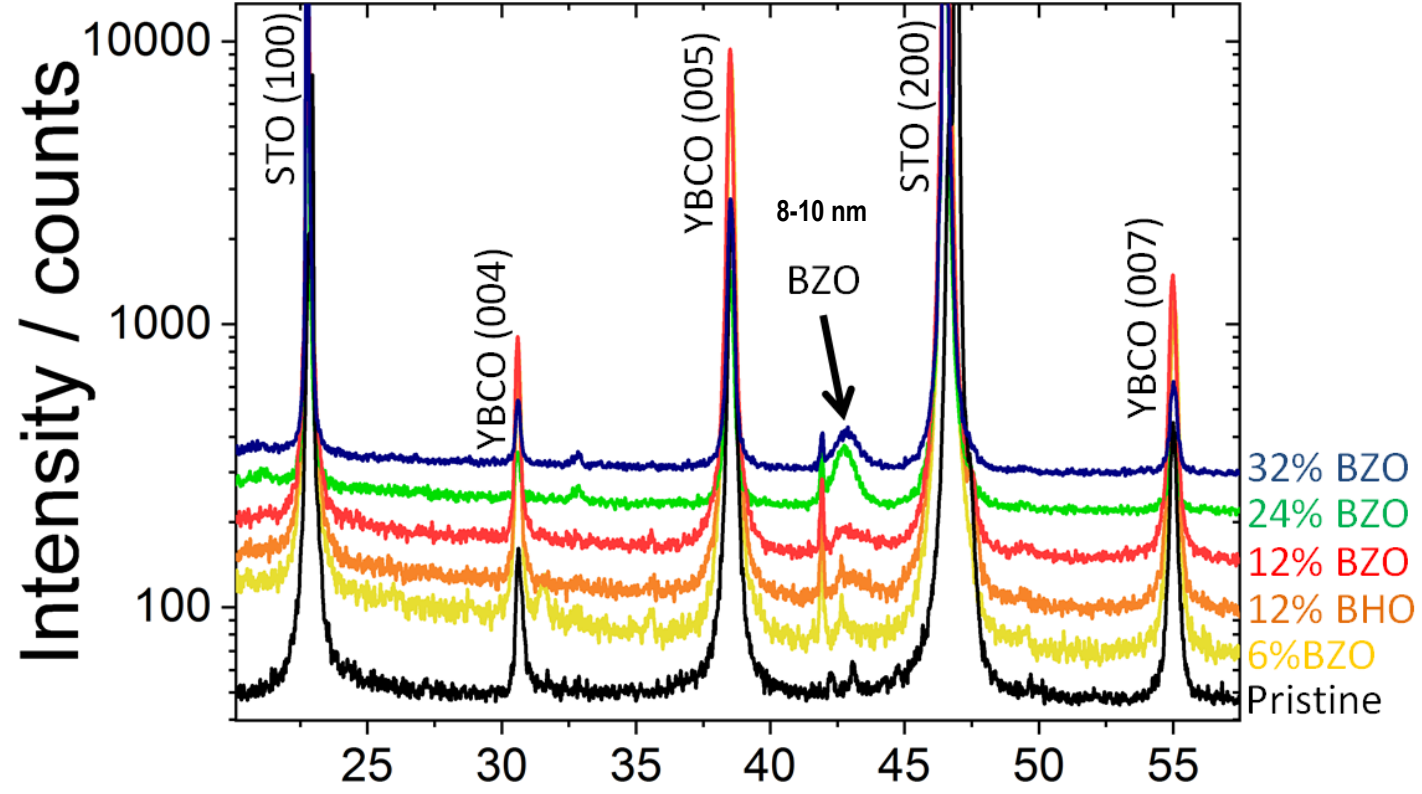
Nanocomposites growth by TLAG-CSD



$$\Delta\phi < 0.8^\circ$$



$$\Delta\omega < 0.6^\circ$$

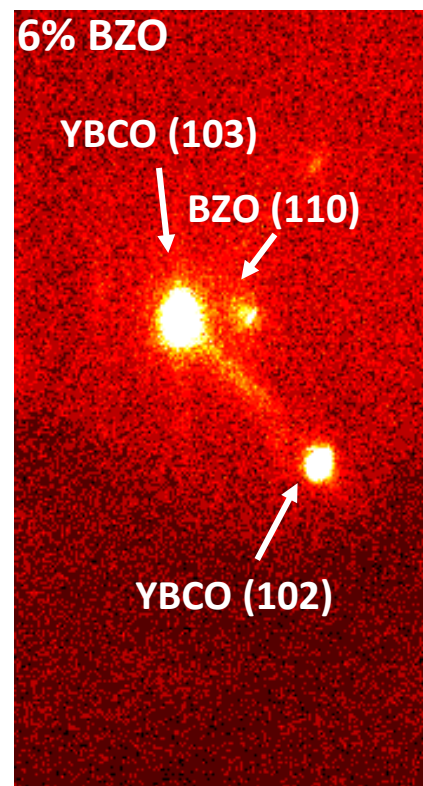
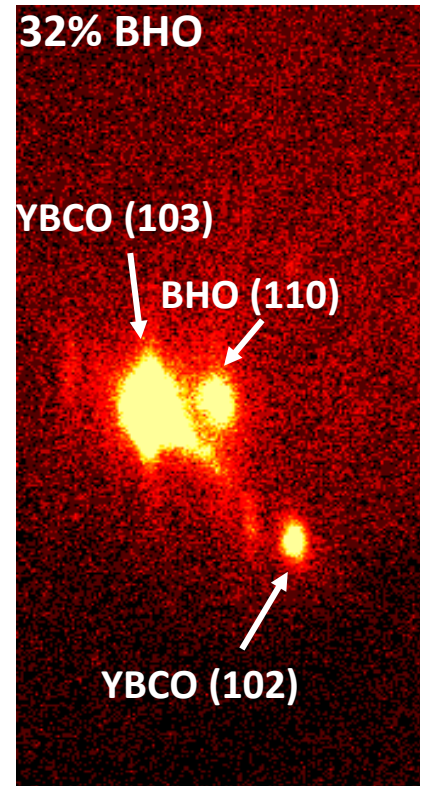


Epitaxial nanoparticles in TLAG-CSD contrary to TFA-CSD

Nanoparticles orientation in TLAG-CSD

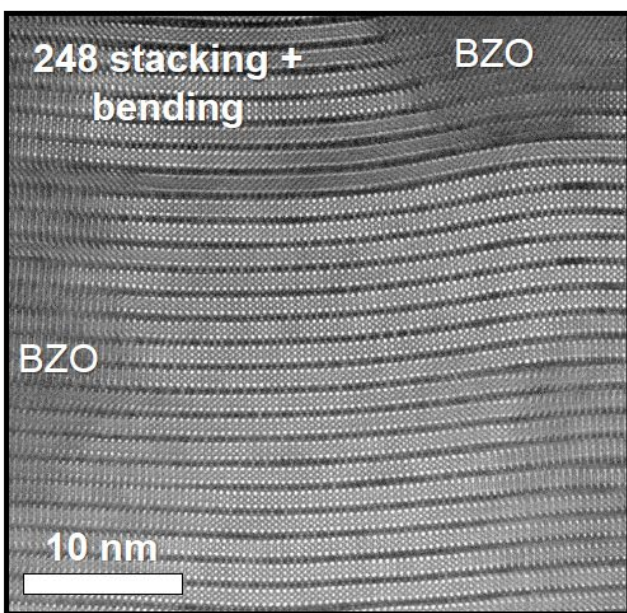
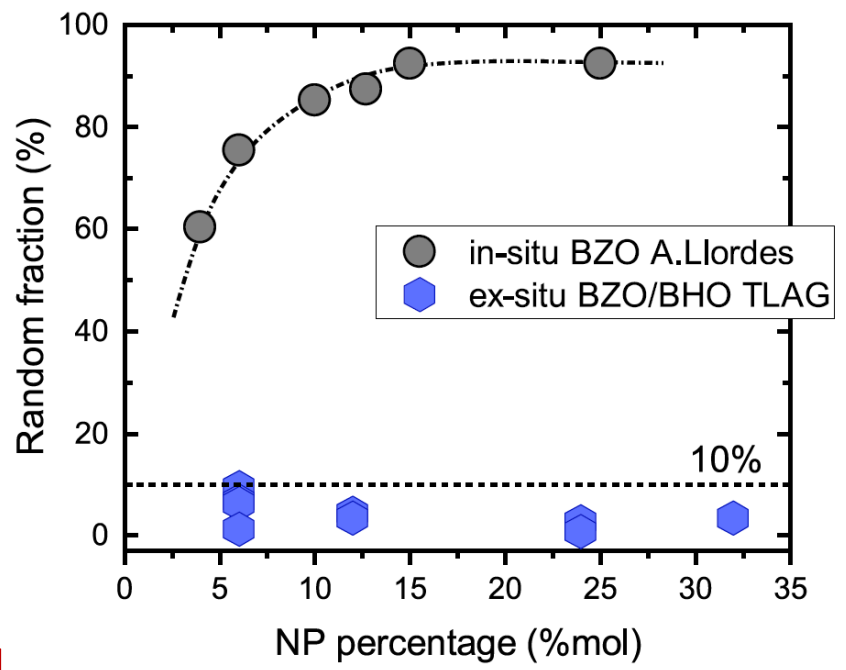
Measurement: chi: 45°, at BZO (110) most intense reflexion

Low PO₂ route



All NPs percentages:
0-10% random orientation

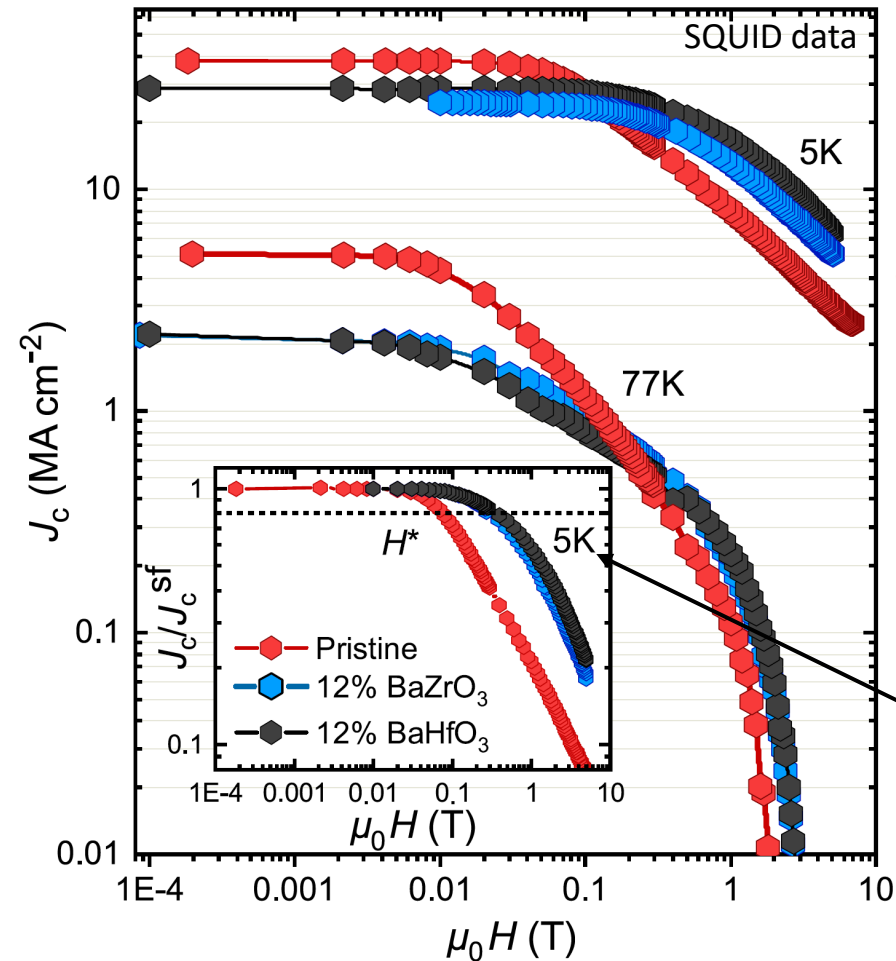
Example of 80% random orientation NPs (TFA)



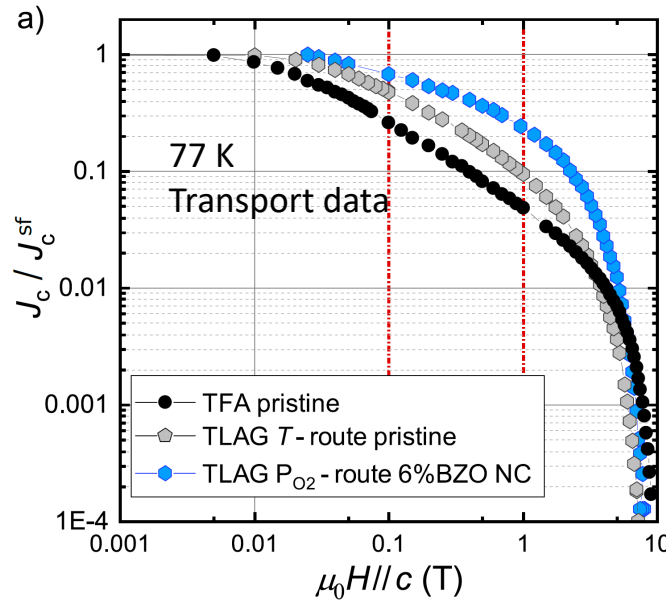
Preformed NPs can rotate within the liquid state to reach epitaxy with YBCO matrix

L. Soler et al, Nat Comm (2020)
J. Banchewski et al, to be published

TLAG-CSD superconducting properties

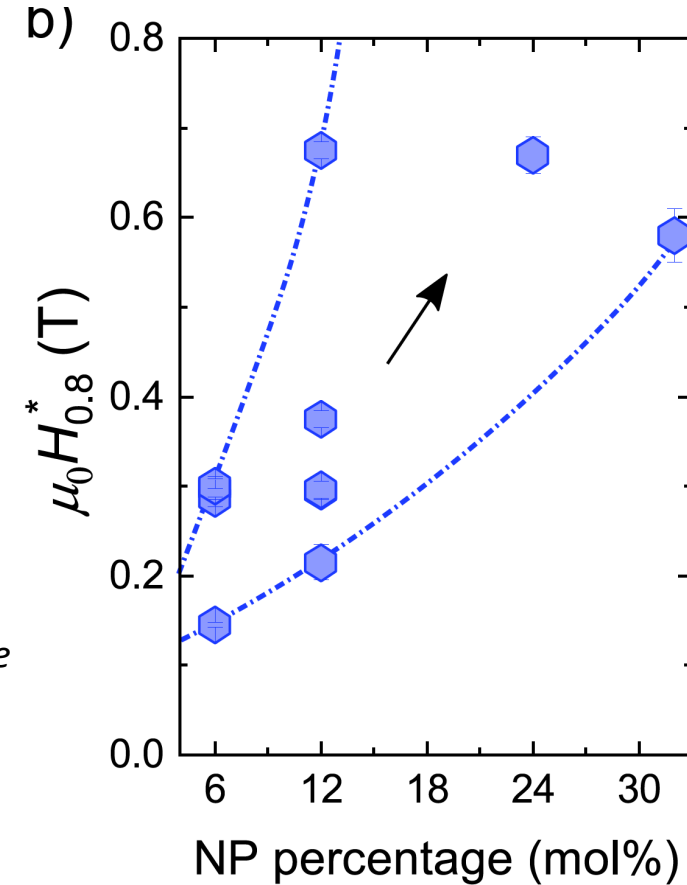


High J_c values with in-field performance of TLAG nanocomposite outperforming pristine films



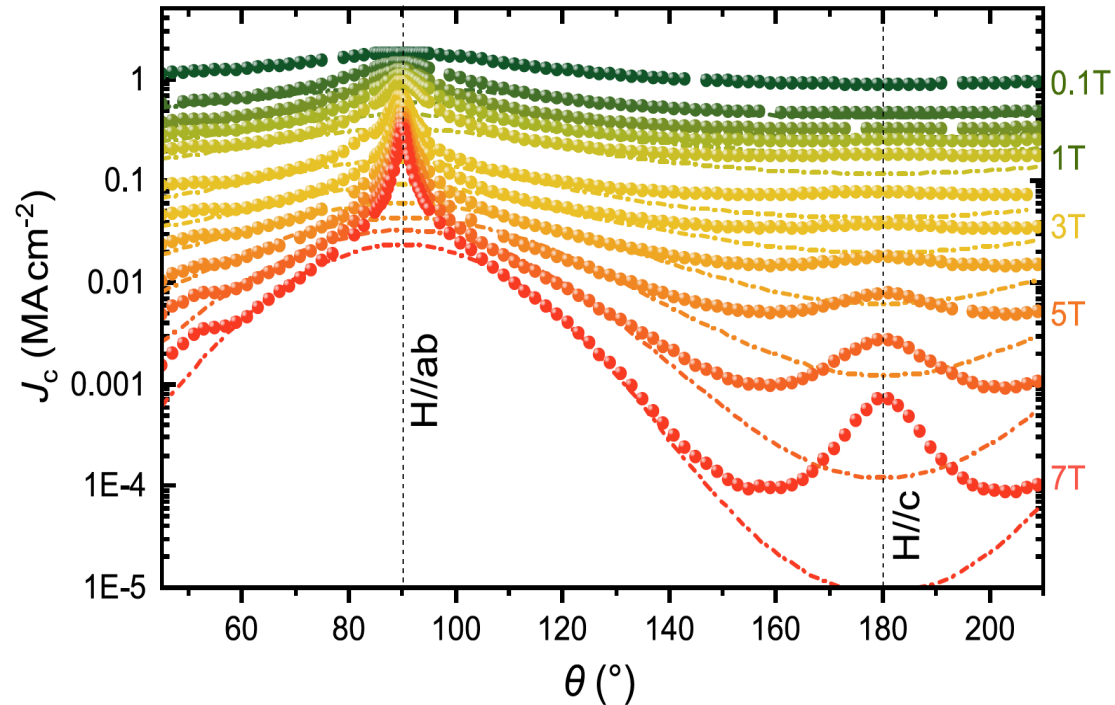
H^* (T): single vortex regime (a measure of the density of pinning centers)

J_c^{sf} constant up to 24 % mol

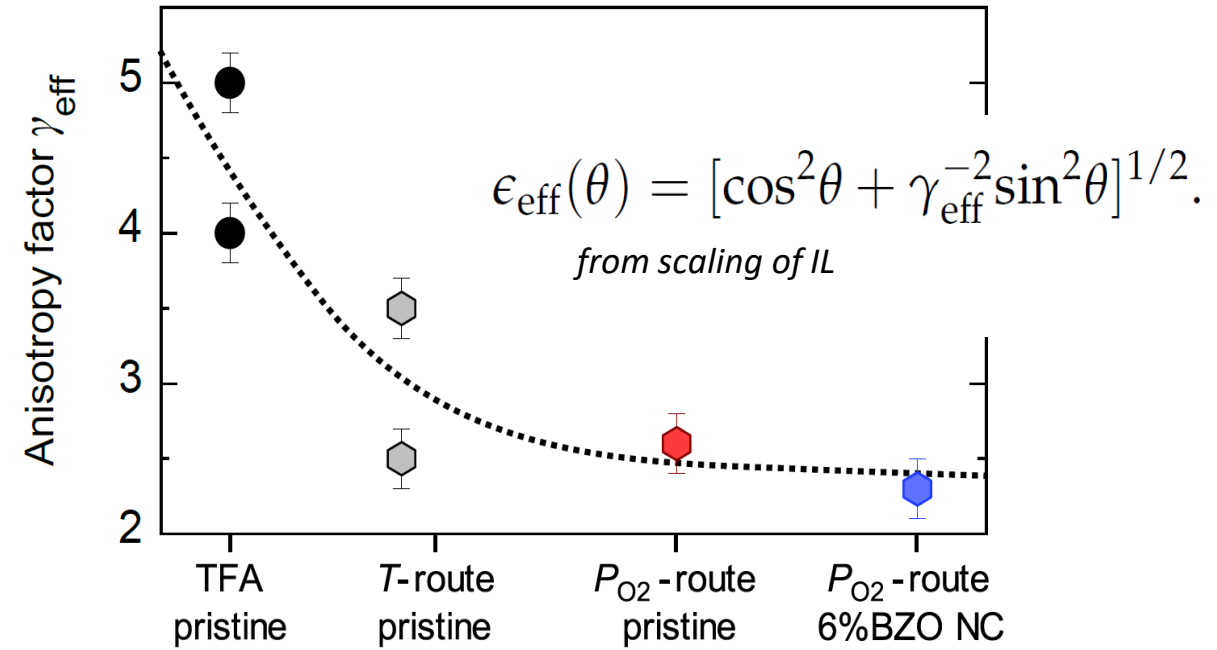


H^* increases with nanoparticles percentage, indicating an increase of vortex pinning centers

TLAG-CSD superconducting properties



Isotropic and anisotropic pinning contributions



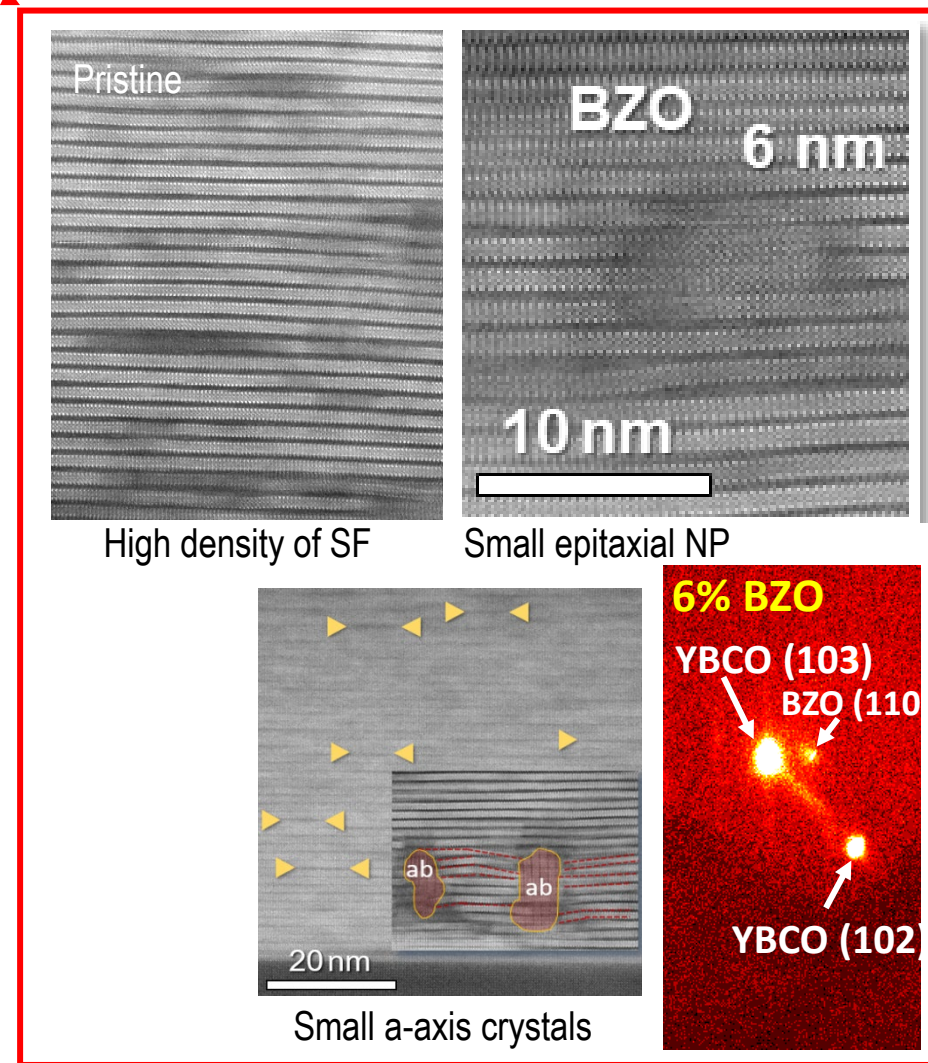
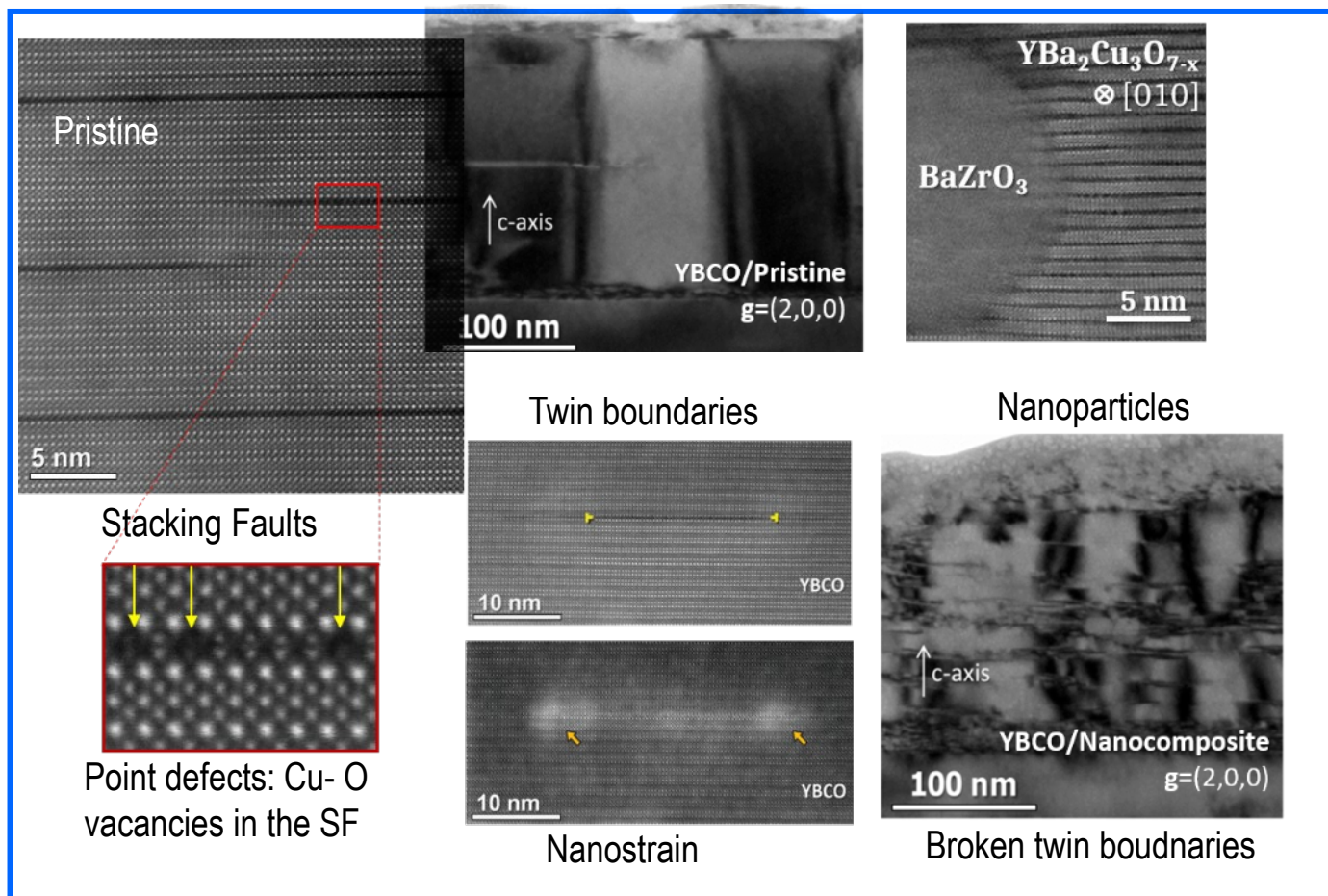
Effective anisotropy decrease due to nanostrain (SFs) and nanoparticles

L. Soler et al, Nature Communications (2020)

J. Banchewski et al, to be published



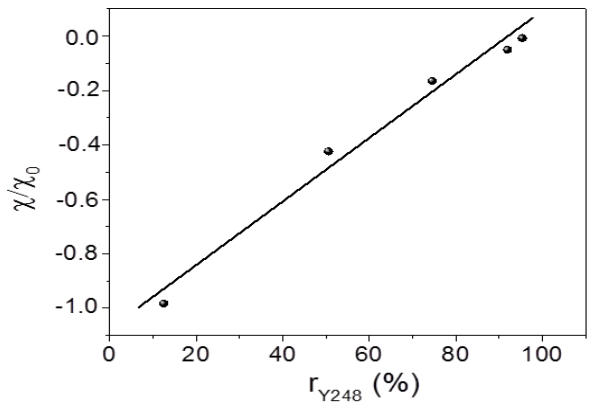
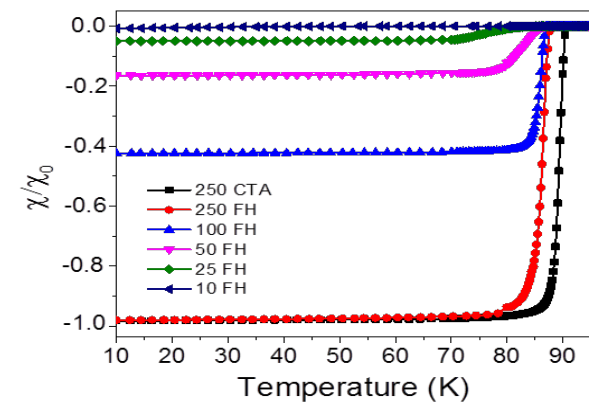
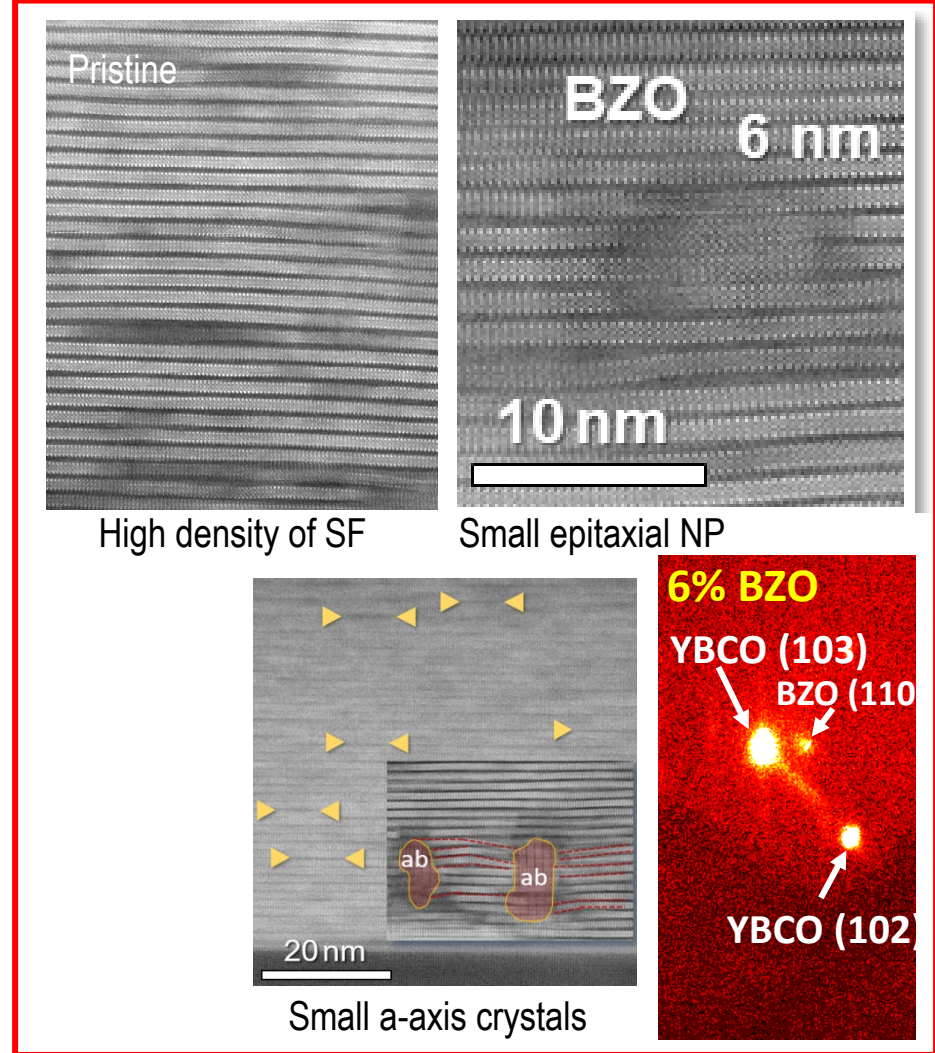
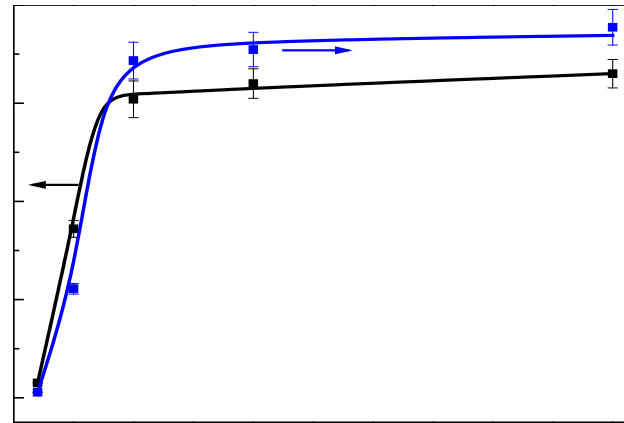
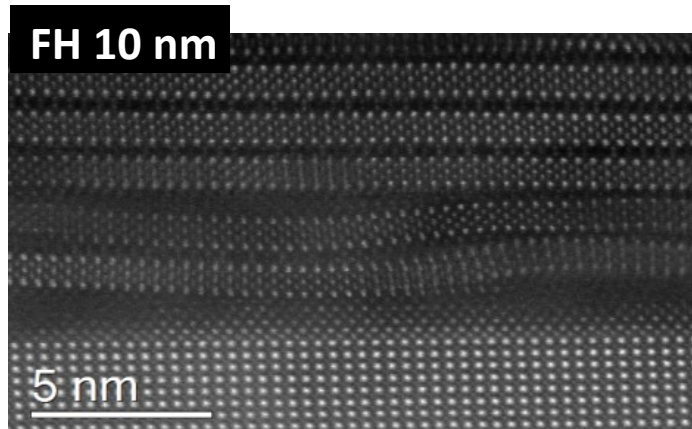
Vortex pinning defects in TFA/TLAG - CSD films



J. Gutierrez et al, Nat Mat (2007)
A. Llordés et al, Nat Mat (2012)
A. Palau et al., SUST (2018)
Z. Li et al, Sci Rep. (2019)
L. Soler et al, Nat Comm (2020)

J. Gazquez et al., Adv. Sci. (2016)
R. Guzman et al, APLMat (2017)
S.T. Hartman et al, PRMat (2019)
Z. Li et al., Nanoscale Adv (2020)

Vortex pinning defects in TFA/TLAG - CSD films



**Defective Stacking
Fault is non-
superconducting**

J. Gutierrez et al, Nat Mat (2007)
 A. Lordés et al, Nat Mat (2012)
 A. Palau et al., SUST (2018)
 Z. Li et al, Sci Rep. (2019)
 L. Soler et al, Nat Comm (2020)
 J. Gazquez et al., Adv. Sci. (2016)
 R. Guzman et al, APLMat (2017)
 S.T. Hartman et al, PRMat (2019)
 Z. Li et al., Nanoscale Adv (2020)

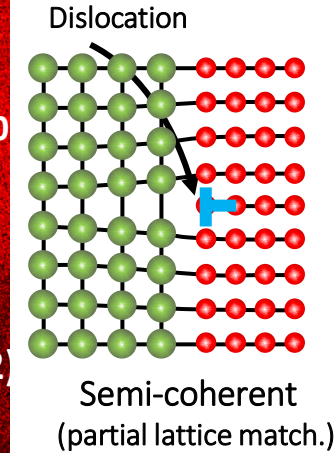
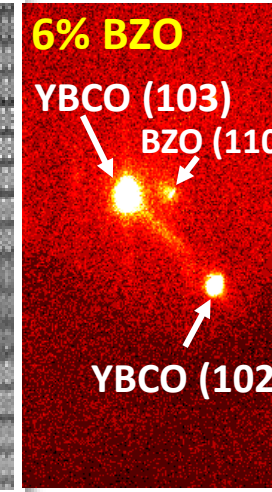
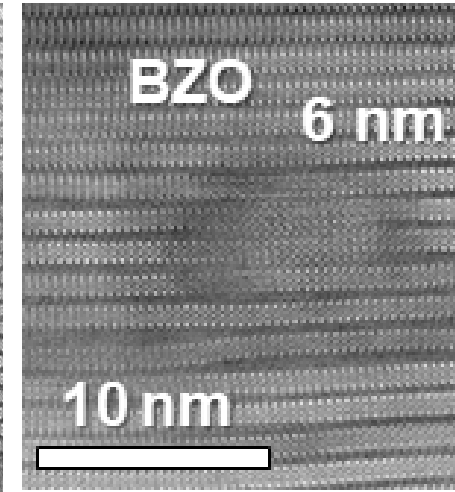
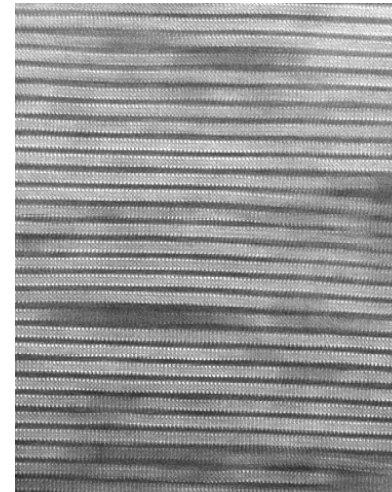
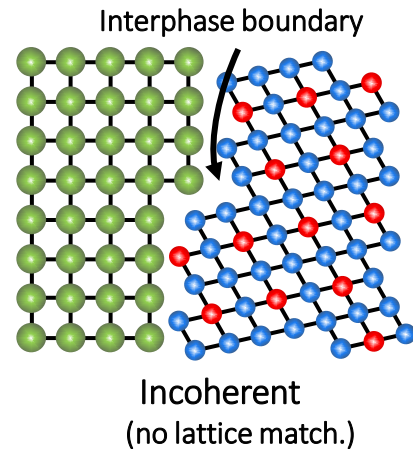
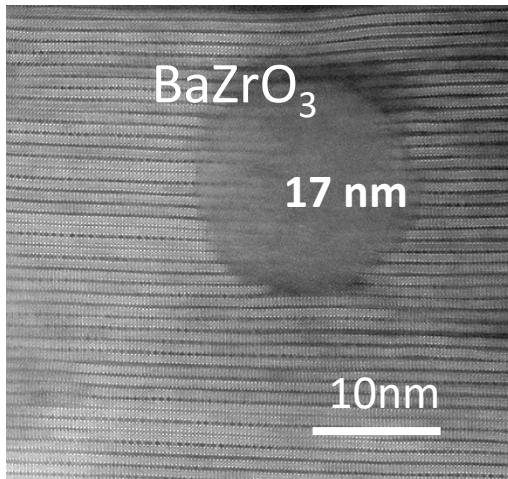
Vortex pinning in TLAG-CSD vs TFA-CSD

TFA-CSD

- Low density of defects in pristine films
- High density of defects achieved in Nanocomposites (NC)
- Nanocomposites contain random NPs that provide higher density of stacking faults (SFs)
- Flash heating provides less NP coarsening in NC

TLAG-CSD

- Pristine TLAG exhibits very high density of defects
- Preformed NPs can rotate within the transient liquid and get embedded epitaxially in YBCO matrix
- Epitaxial NPs in NC do influence little the density of SFs
- Epitaxial small NPs act as core pinning centres, increasing the overall pinning properties

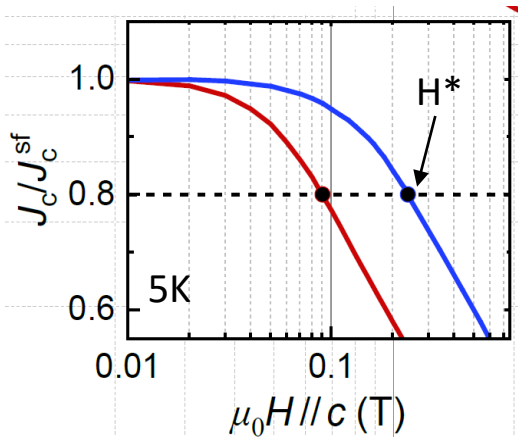


J. Gutierrez et al, Nat Mat (2007)
 A. Llordés et al, Nat Mat (2012)
 Z. Li et al, Sci Rep. (2019)
 A. Palau et al., SUST (2018)
 Z. Li et al., Nanoscale Adv (2020)

L. Soler, Nat Comm (2020)

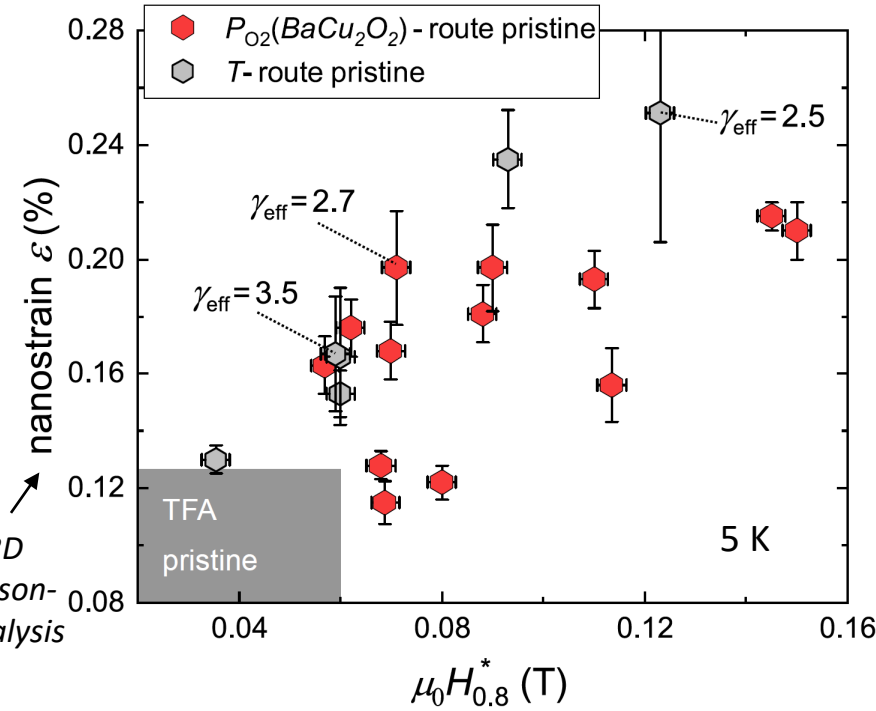
TLAG-CSD is a very promising process to obtain high vortex pinning films

Vortex pinning in TLAG-CSD films and nanocomposites

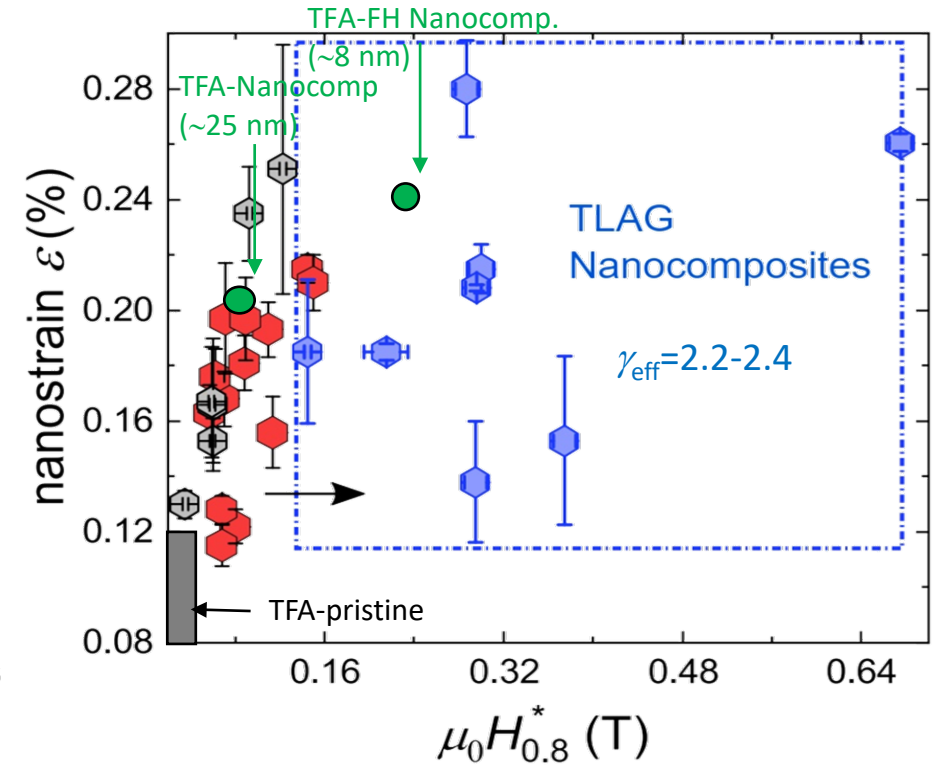
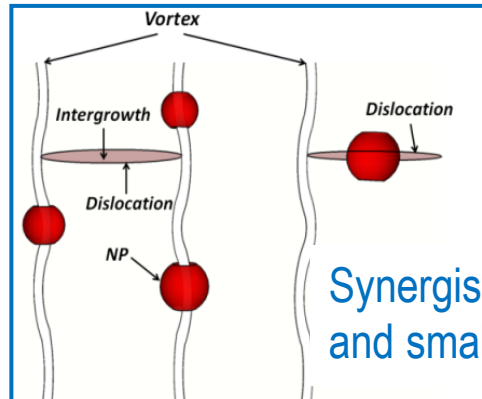


H^* : single vortex regime (measure of the density of pinning centers)

from XRD
Williamson-Hall analysis



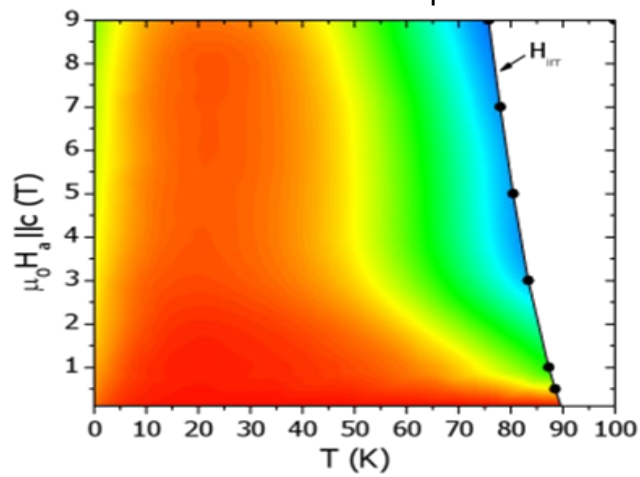
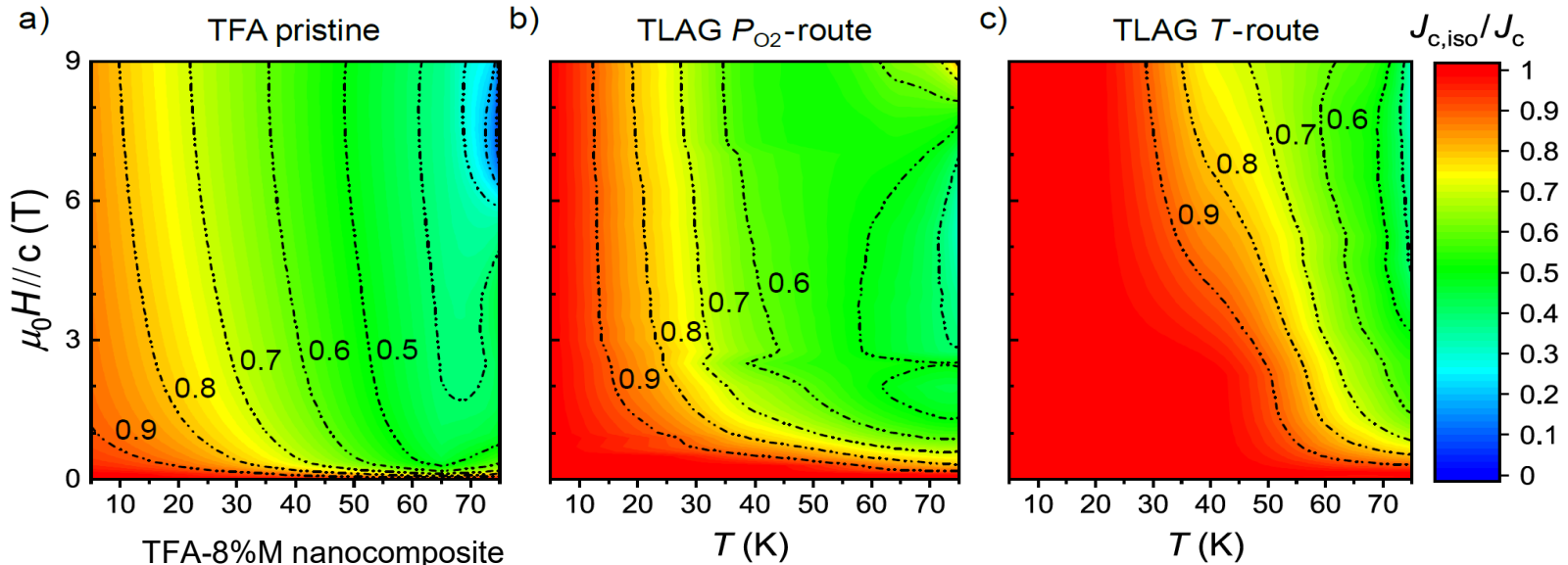
Strong increase of H^* with nanostrain and very low anisotropy in pristine films



Outstanding values of H^* with low anisotropy in nanocomposite films suggests additional pinning contribution from small NPs which can be included in a higher concentration

Pinning contributions of TLAG-CSD

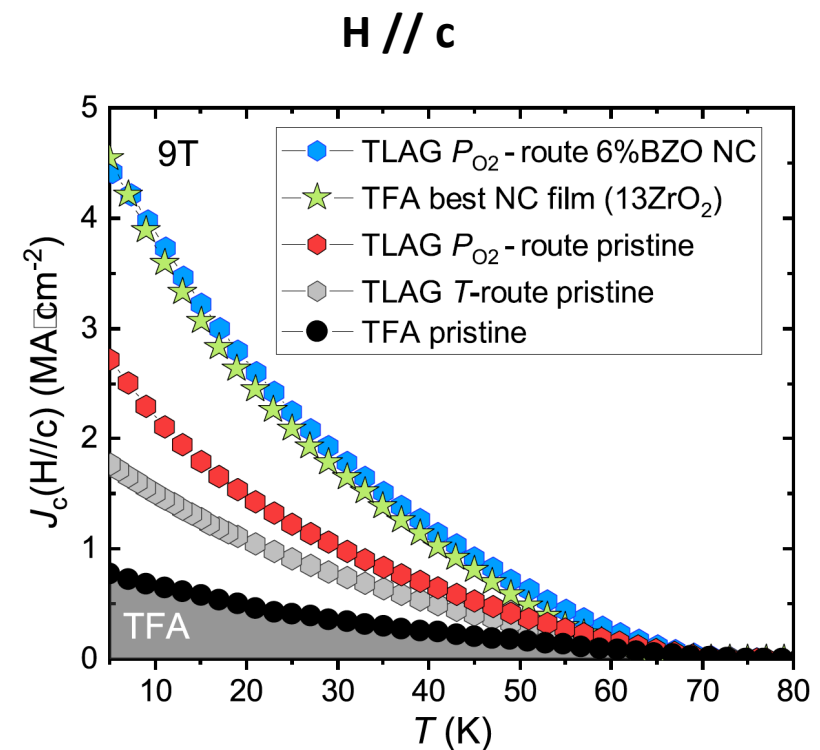
Isotropic-Strong pinning contribution



$$J_c(T) = J_c^{\text{iso-wk}}(T) + J_c^{\text{iso-str}}(T) + J_c^{\text{aniso-str}}(T)$$

Strong-isotropic pinning contribution of pristine TLAG emulates TFA-nanocomposite

- Enhanced nanostrain in pristine TLAG
- TLAG nanocomposites display high vortex pinning



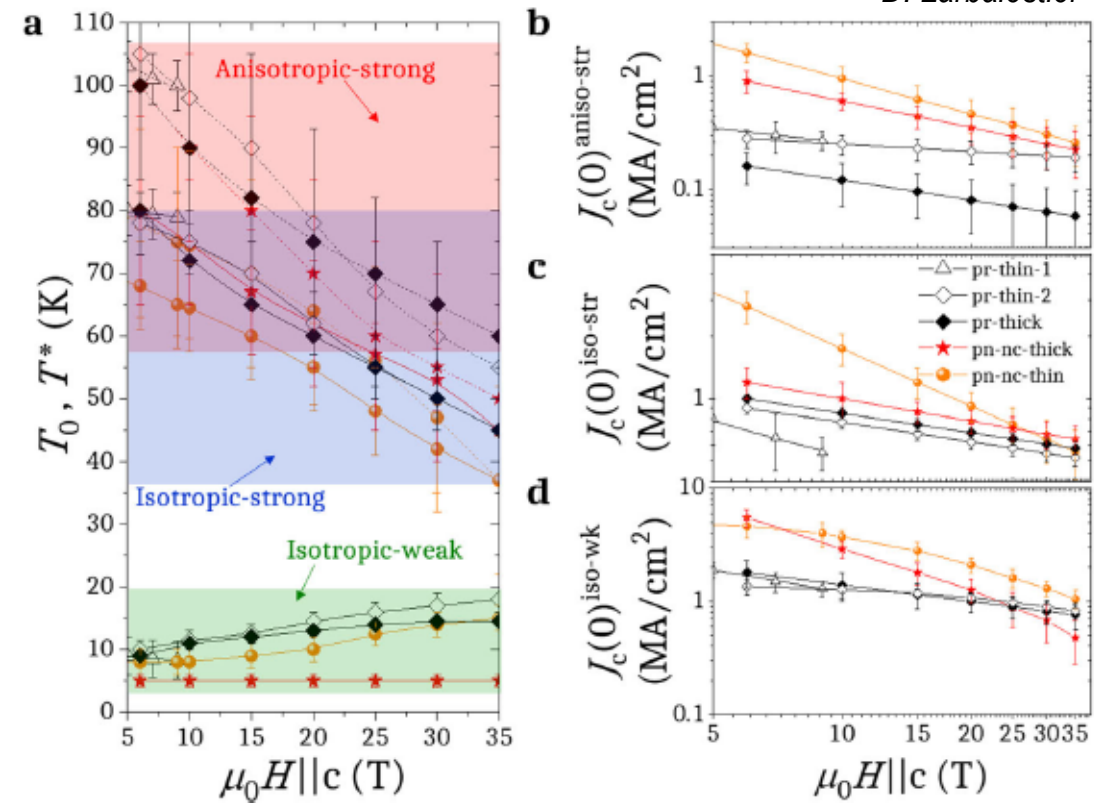
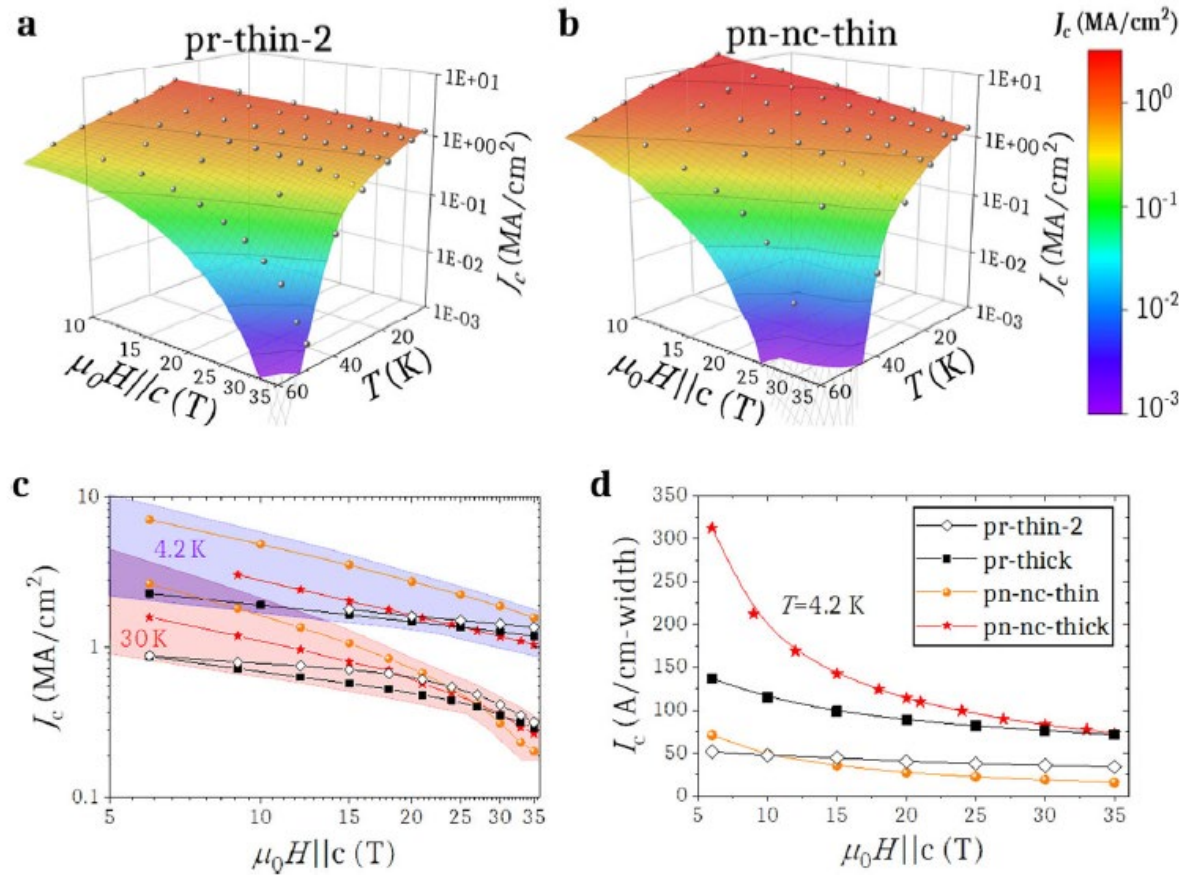
High field properties of nanocomposites similar for TFA and TLAG



Pinning landscapes in nanocomposite films: very high magnetic fields

$$J_c(T) = J_c(0)^{\text{iso-wk}} \exp(-T/T_0) + J_c(0)^{\text{iso-str}} \exp(-3(T/T_0^{\text{iso-str}})^2) + J_c(0)^{\text{aniso-str}} \exp(-3(T/T_0^{\text{aniso-str}})^2)$$

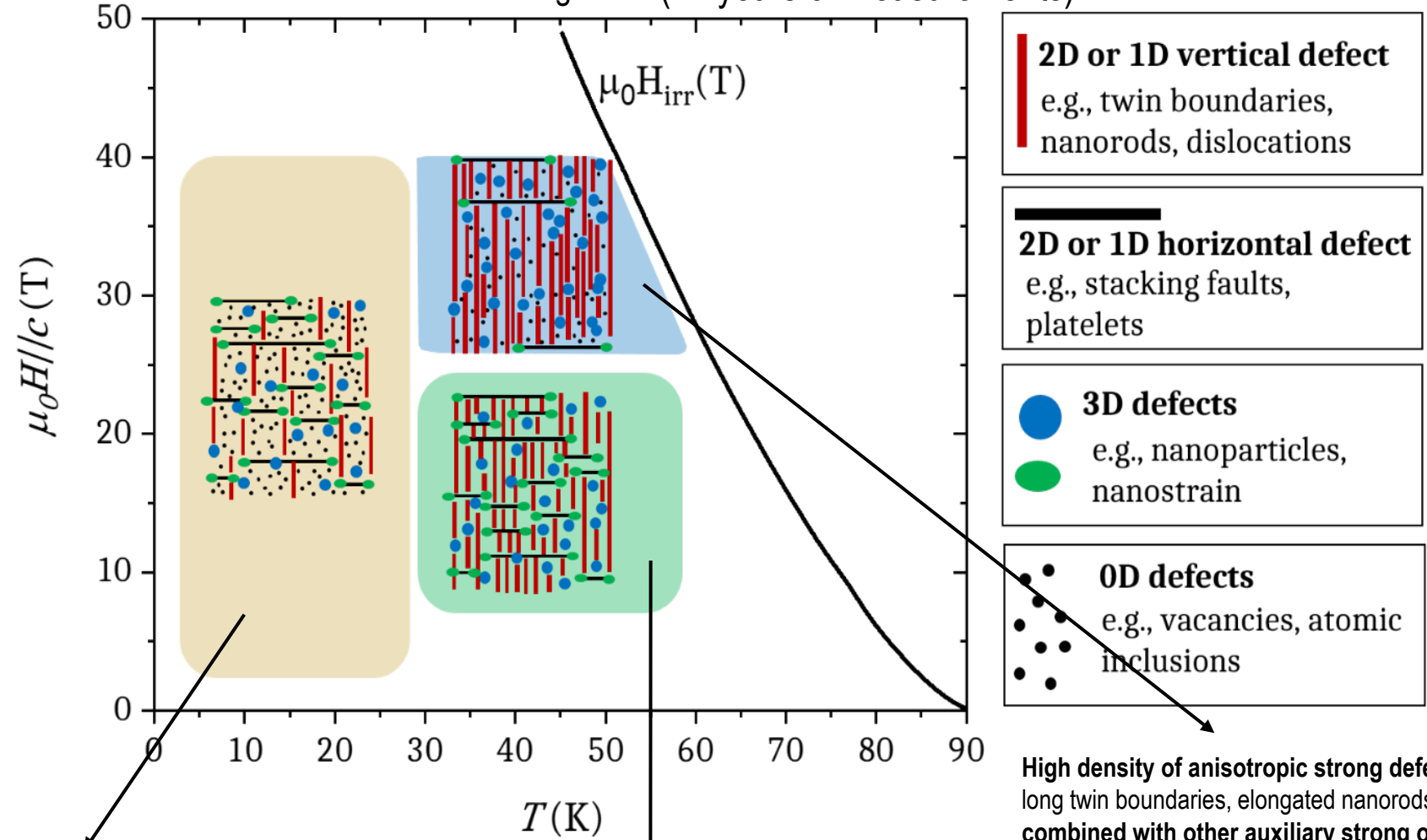
D. Abraimov
J. Jaroszynski
D. Larbalestier



Optimized pinning landscapes in CSD nanocomposite films

D. Abraimov
J. Jaroszynski
D. Larbalestier

Low and intermediate T - Intermediate and high H (14 years of measurements)



2D or 1D vertical defect
e.g., twin boundaries, nanorods, dislocations

2D or 1D horizontal defect
e.g., stacking faults, platelets

3D defects
e.g., nanoparticles, nanostrain

0D defects
e.g., vacancies, atomic inclusions

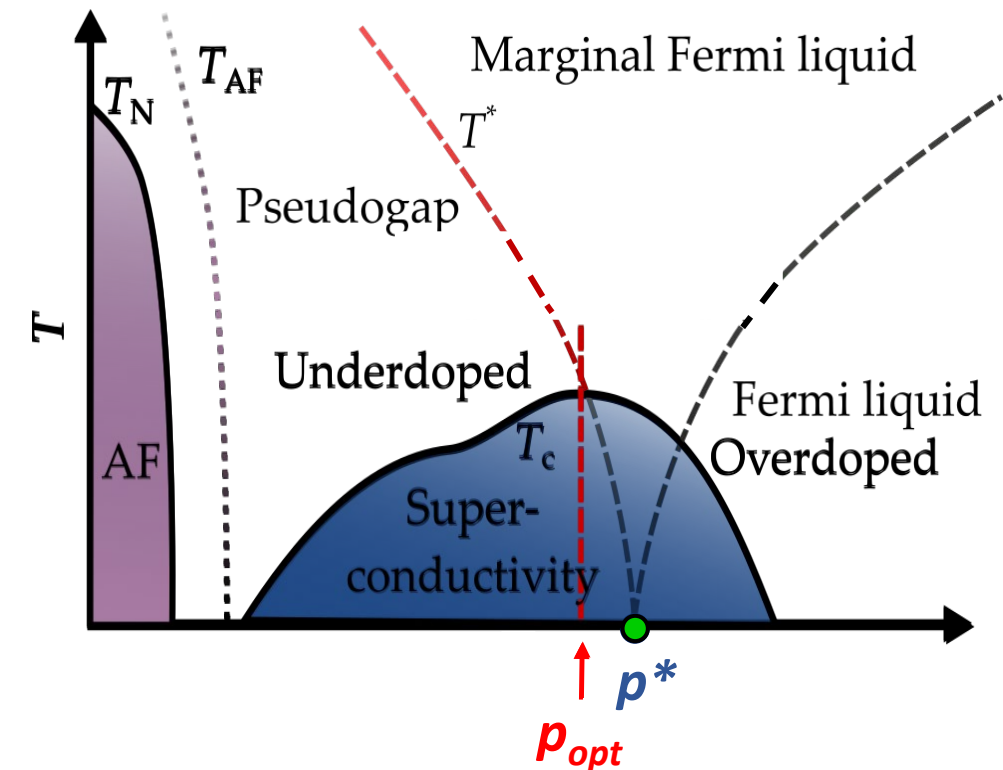
High density of anisotropic strong defects with very long vertical coherence: long twin boundaries, elongated nanorods, thick CSD nanocomposites combined with other auxiliary strong or weak isotropic defects to lessen vortex creep excitations (1D-2D mandatory but all defects will help to diminish creep)

High density of isotropic defects: Cu-O vacancies, short SF, small NP (better Np than nanorods)

Large density of strong isotropic and anisotropic defects with long vertical coherence: nanoparticles, nanostrain, long nanorods, long twin boundaries (Nanorods and nanoparticles will add effects)



Tune charge carrier density by oxygen overdoping



$p_{opt} = 0.16$ holes/ CuO_2 -plane: optimal doping for maximum T_c

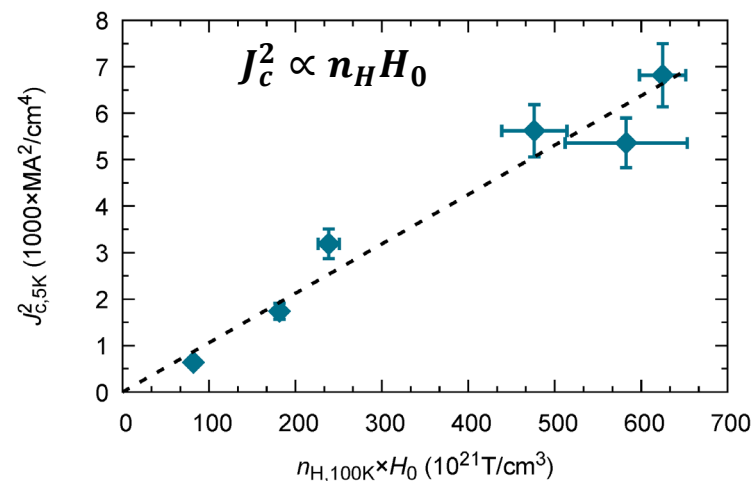
$p^* = 0.19$ holes/ CuO_2 -plane: Critical doping (QCP)

$$\text{Pinning force } F_p = \sum_i^{N_p} f_{p,i}(B, T) \propto J_c$$

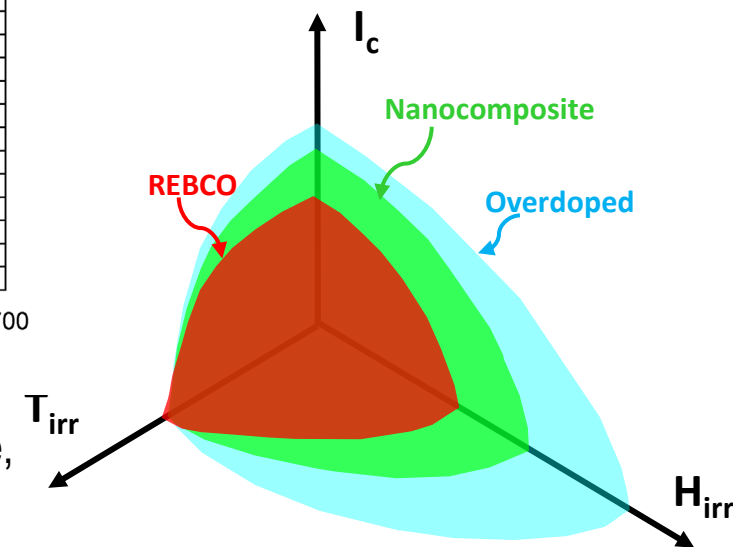
$$f_p \propto E_c \text{ condensation energy}$$

$$J_d^2 \propto n_s E_c \longrightarrow J_c^2 \propto n_H H_0 \text{ (} H_0 \text{ from in-plane magnetoresistance)}$$

(three independent experimental parameters)

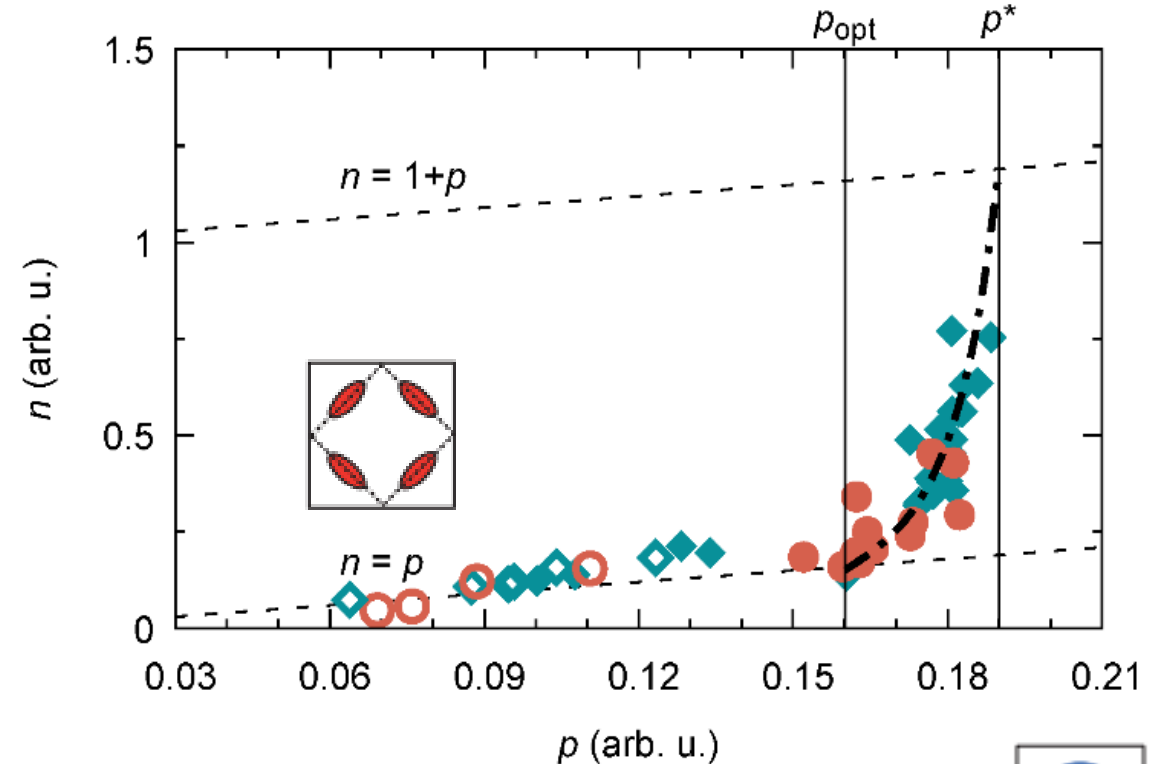
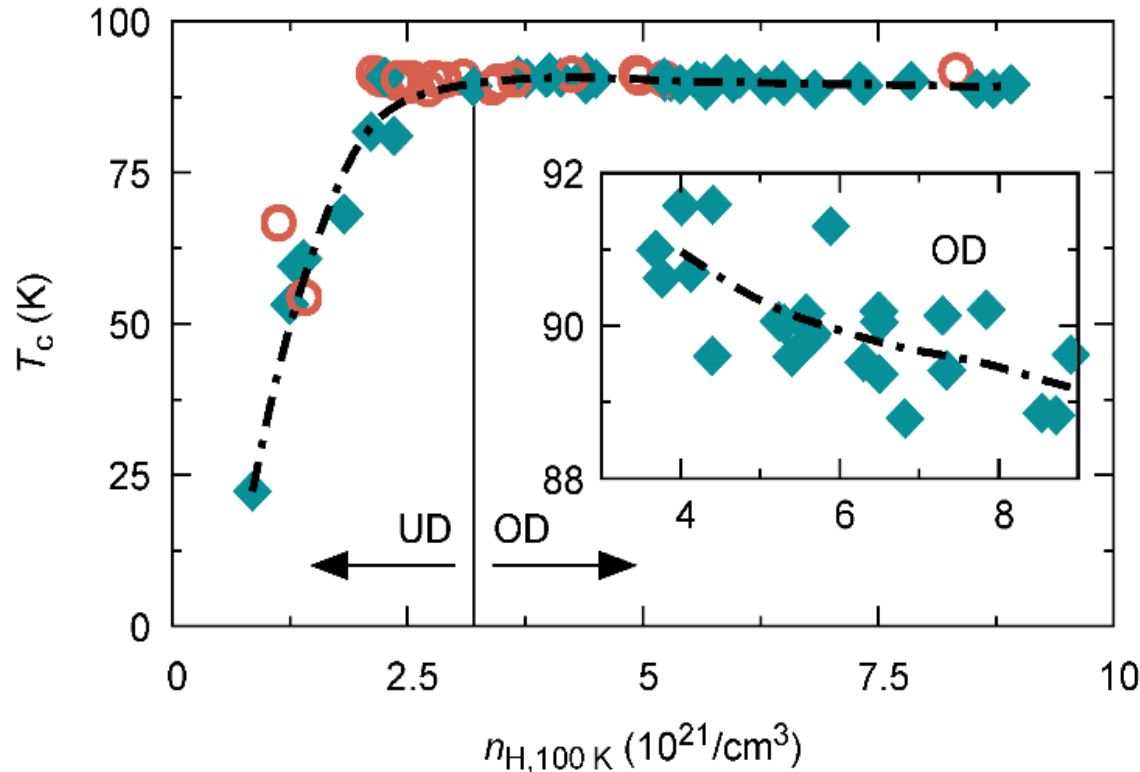


n_H and E_c increases in the overdoped state, and consequently J_c should increase



Carrier concentration effects: oxygen overdoping

YBCO PLD and TFA – CSD thin films

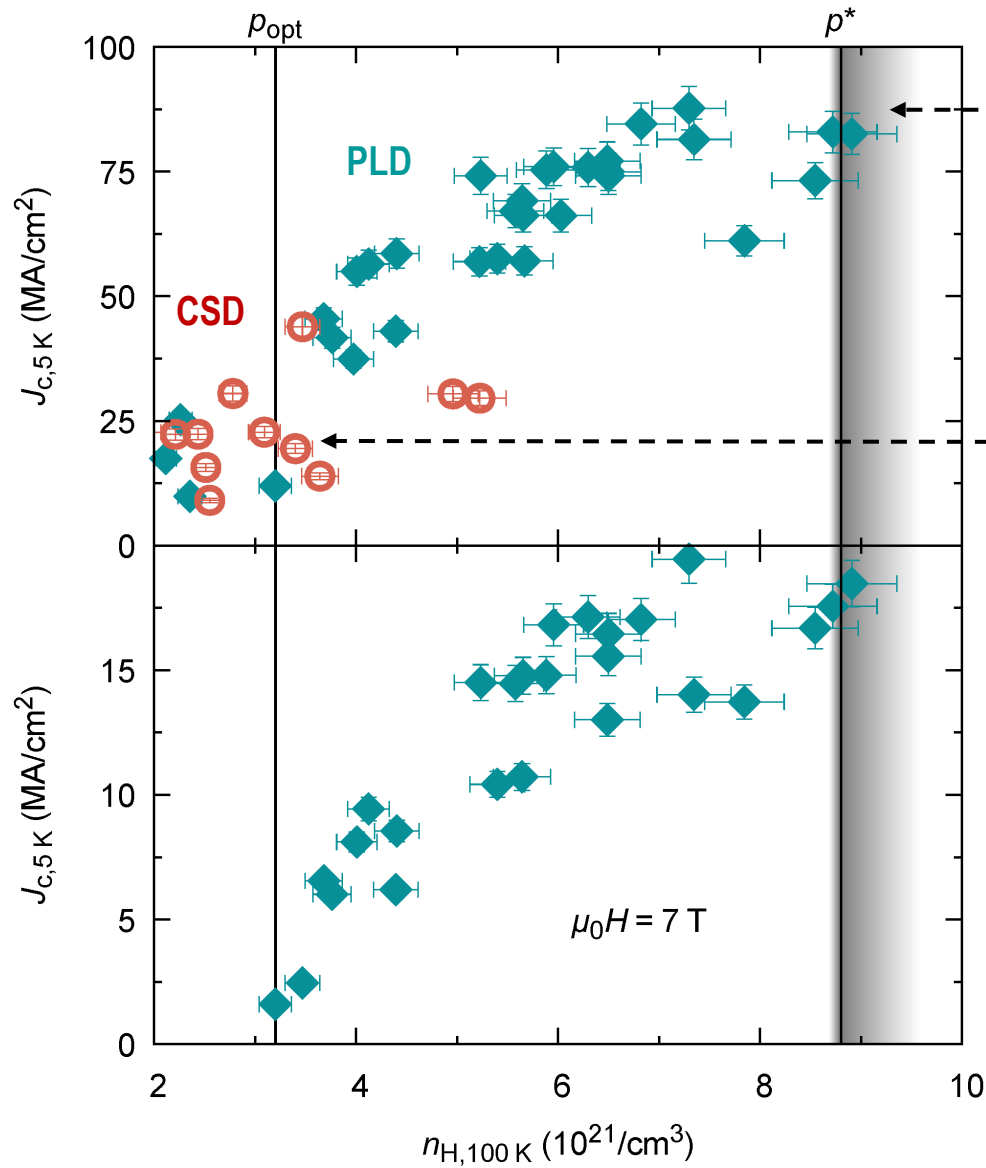


- Carrier concentration determined by Hall effect (100 K)
- Overdoping is achieved by oxygen excess

- Fermi surface reconstruction at the Quantum Critical Point ($p^* > p_{opt}$): large increase of the carrier density n (cylindrical Fermi surface)
- Non-unique relation between the charge carrier density n and doping, p .



Strong increase of J_c in the overdoped state



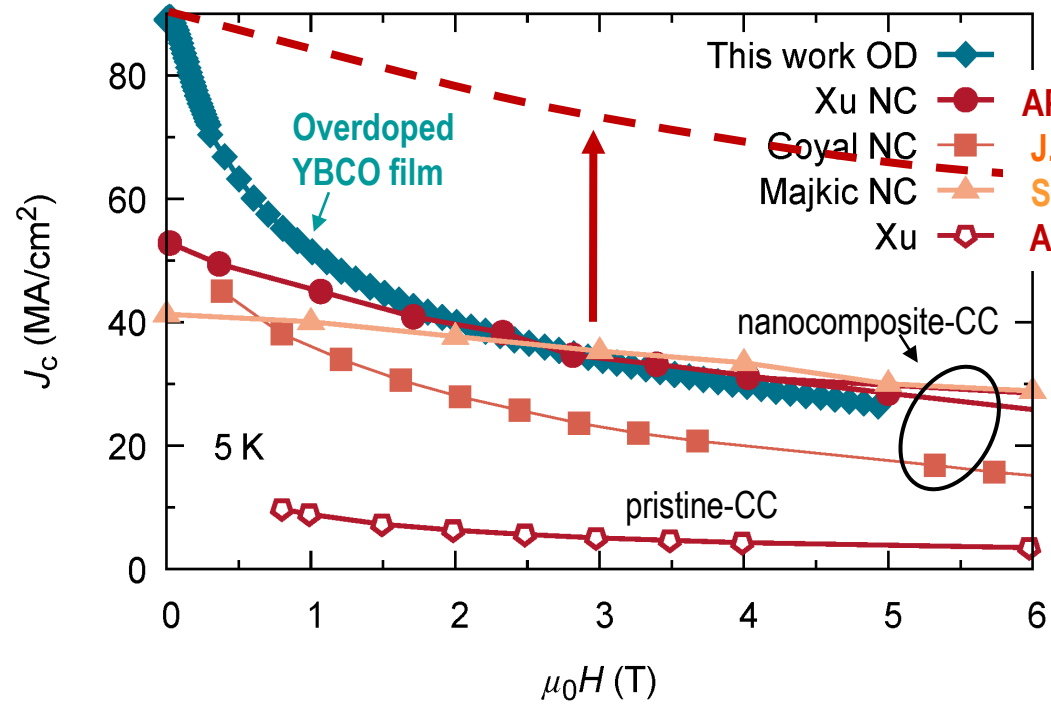
$$J_c(p^*) \approx \frac{1}{5} J_d(p^*) = 90 \text{ MA/cm}^2$$

$$J_d(p^*) \approx 500 \text{ MA/cm}^2$$

Strong increase of J_c with n_H
(x4 from p_{opt} to p^*)

$$J_c(p^{opt}) \approx \frac{1}{10} J_d(p^{opt})$$

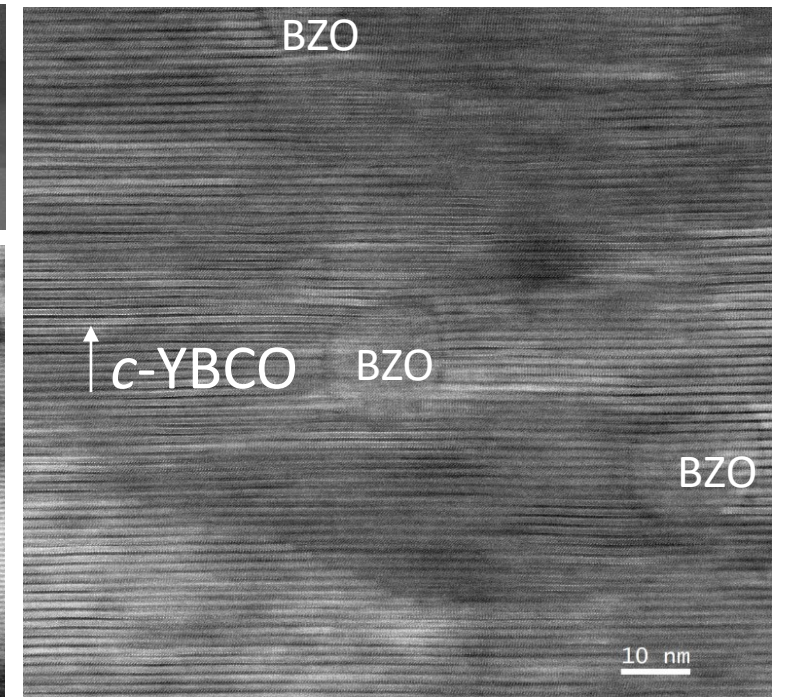
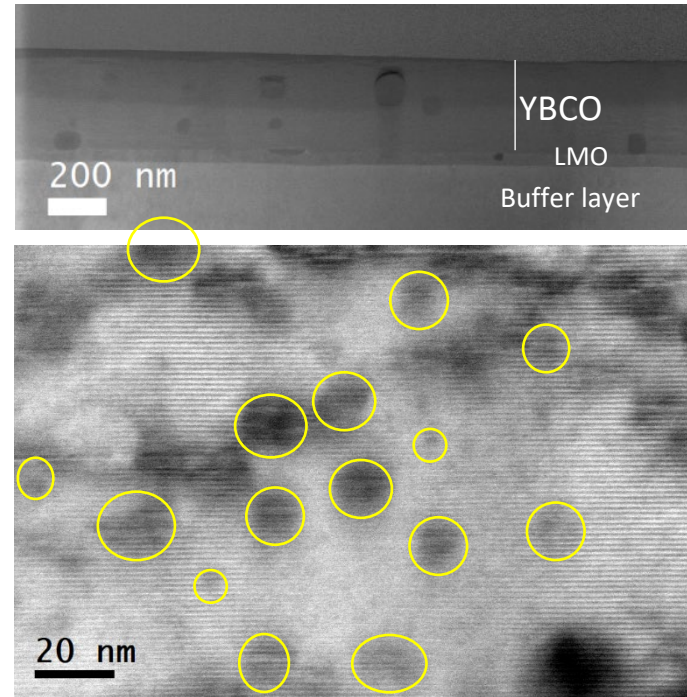
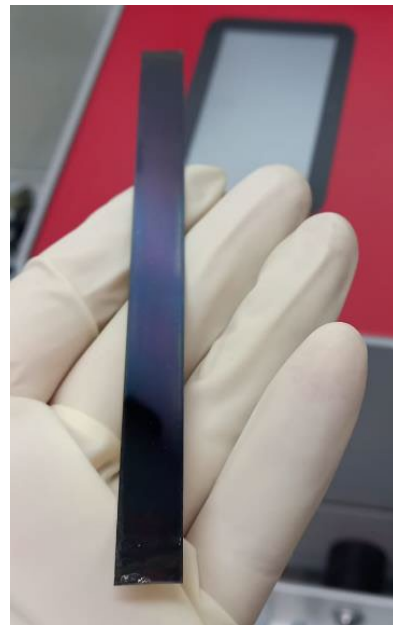
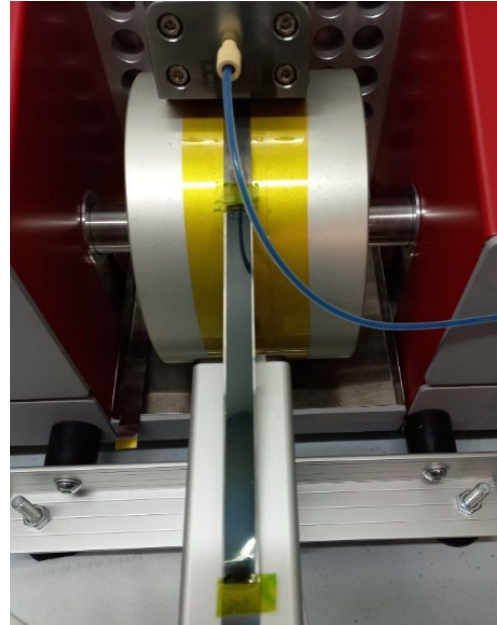
$$J_d(p^{opt}) \approx 330 \text{ MA/cm}^2$$



Overdoping is a robust method to reach ultrahigh $J_c(H)$

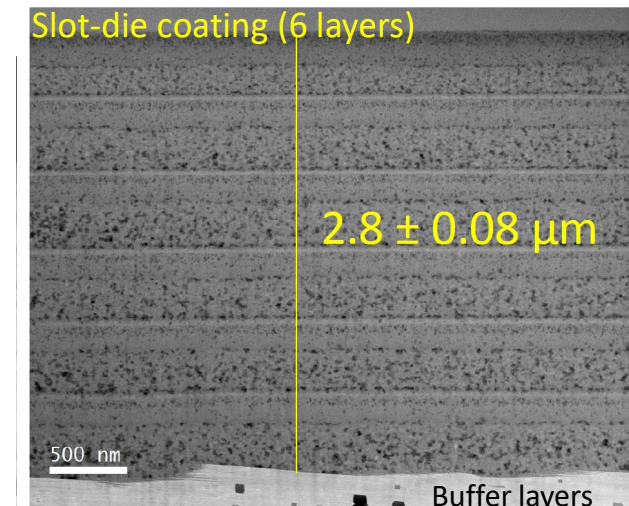
YBCO TLAG-CSD NANOCOMPOSITE FILMS

Extended to technical substrates
in collaboration with



450 nm films

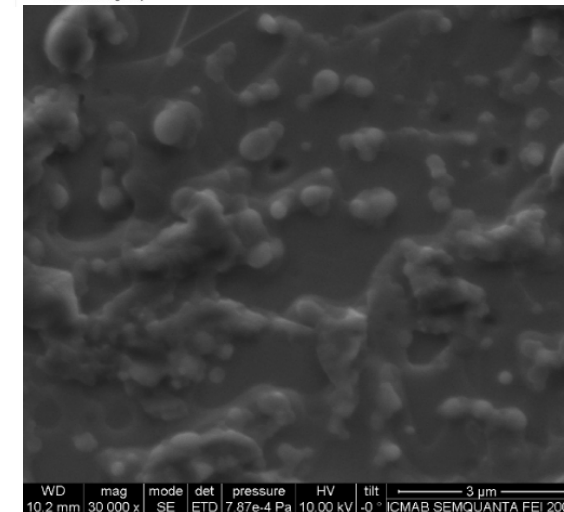
$$J_c(5K) = 24 \text{ MA/cm}^2 \quad J_c(77K) = 2 \text{ MA/cm}^2$$



TLAG-CSD Coated Conductors

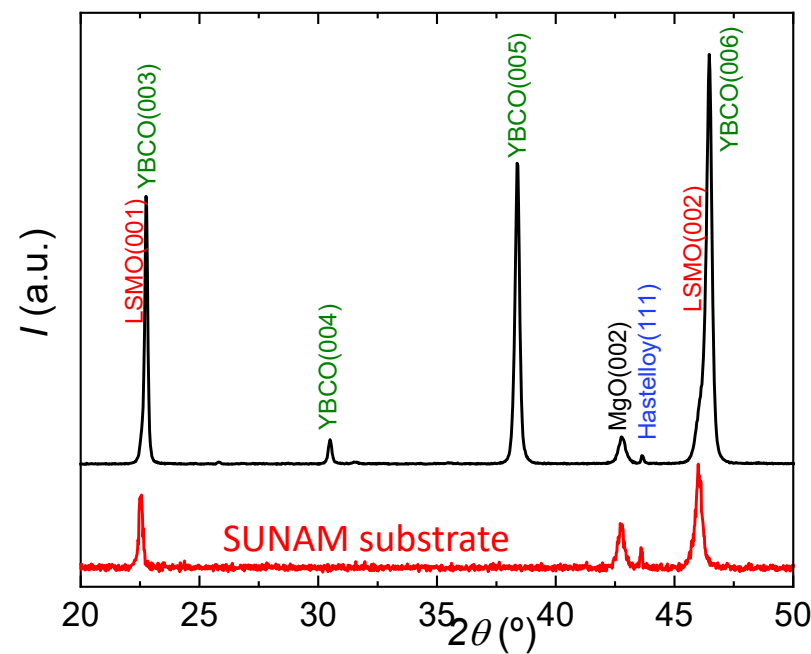
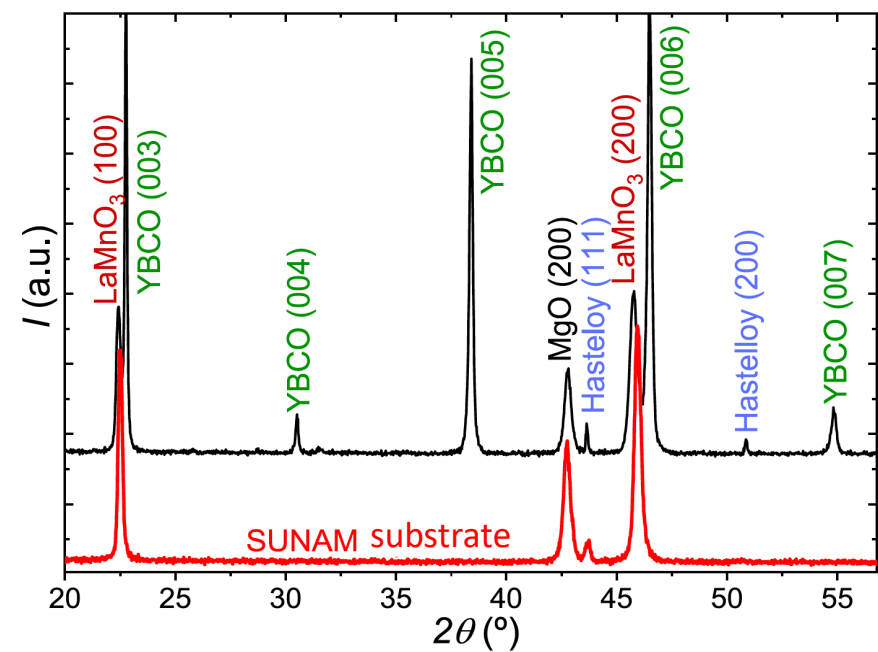


EXCELENCIA SEVERO OCHOA



5 cm test samples of 1 μm thick homogeneous pyrolyzed YBCO deposited on SuNAM substrates

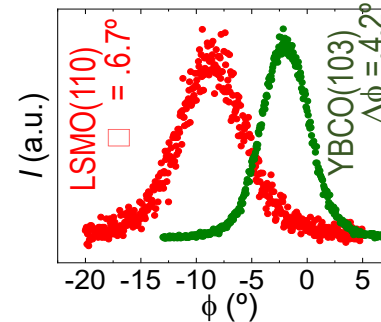
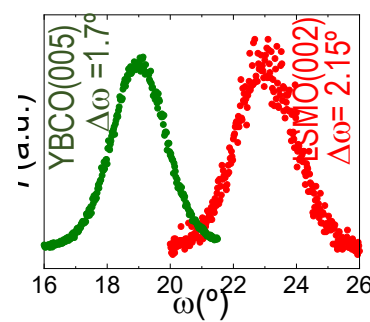
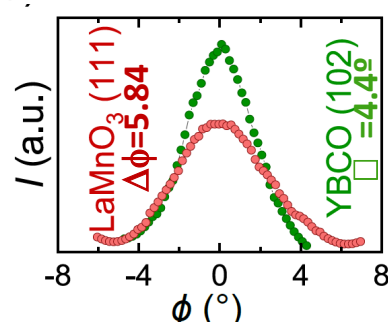
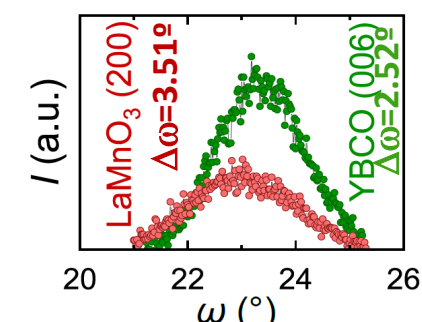
Liquid growth morphology, very high epitaxy and texture quality, with a noticeable improvement of texture of the YBCO layer



$T_c = 90 \text{ K}$
 $J_c (77 \text{ K}) = 2 \text{ MA/cm}^2$
 $J_c (5 \text{ K}) = 23 \text{ MA/cm}^2$

Need to further reduce some secondary phases interrupting current percolation: tuning process conditions

Several different metallic substrates tested successfully



Advantages TLAG-CSD vs TFA-CSD

	TFA-CSD	TLAG-CSD
Growth mechanism	Gas-solid	Liquid-solid
Growth rate	Slow (~1 nm/s)	Ultrafast (~100-1.000 nm/s)
Supersaturation control	P_{H_2O} , T	[Y], Liquid composition, T, PO_2
C-axis window	narrow	Wide and versatile (T and PO_2 routes)
Nanocomposites	Spont. Segregat., preformed nanoparticles	Preformed nanoparticles
Nanoparticles orientation	Random	Epitaxial
Pinning centers	Nanostrain, np	Nanostrain, np, new possible defects
H^* (single vortex pinning)	100 mT (200 mT in FH-NC)	600 mT in NC
J_c (77K) / I_c (77K)	2 - 5 MA/cm ² (thin film) / 600 A/cm-w	2 - 5 MA/cm ² (thin film) / 150 A/cm-w
Heating rate	Low (coarsening) or Flash Heating	High (no coarsening)
Cap layer and reactivity	CeO ₂ , weak reactivity	LMO, LSMO, no or weak reactivity
Thickness (Multideposition compatible)	Single deposition : ~ 0.8 - 1 μm Multideposition: ~ 2.5 μm	Single deposition : ~ 0.5 μm Multideposition: ~ 1.5 μm
Large scale manufacturing	Limited volume / complex furnaces	Higher throughput / simplified furnaces

CONCLUSIONS



- TLAG-CSD is a novel low cost and ultrafast film growth methodology.
- Stable, reproducible multifunctional non-fluorine propionate inks have been developed.
- Knowledge of kinetic phase diagrams is essential: outlined through in-situ synchrotron X-ray diffraction.
- T and PO₂-routes processing paths are based on a fast kinetically-controlled formation of a Ba-Cu-O transient liquid.
- TLAG-CSD nanocomposites with preformed nanoparticles lead to outstanding vortex pinning properties. Epitaxial nanoparticles and a high concentration of intergrowths are generated.
- Several industrially produced CC metallic substrates have been tested successfully.
- TLAG-CSD is foreseen as a game changing high throughput R2R CC manufacturing process.